REMARKS

Status of Claims

Other than a formatting change to claim 1, claims 1-13 remain presented for examination without change.

Claim Interpretation

The term "characteristic kinetic quantity of a chemical reaction" has not been defined by Applicmts, therefore it is interpreted as any measurable variable.

The term "species including at least one fluorophore" is interpreted as any molecule which comprises at least one fluorophore, involved in any chemical reaction.

Claim Rejections - 35 USC § 112

The following is a quotation of the first paragraph of 35 U.S.C. 112:

The specification shall contain a written description of the invention, and of the manner and process of making and using it, in such full, clear, concise, and exact terms as ***to enable any person skilled in the art*** to which it pertains, or with which it is most nearly connected, ***to make and use the same*** and shall set forth the best mode contemplated by the inventor of carrying out his invention.

Claims 1-13 are rejected under 35 U.S.C. 112, first paragraph, because the specification, while being enabling for monitoring chemical reactions in which the chemical species are fluorophores themselves and in which the physical or chemical properties of the fluorophores are changed upon irradiation with light in such a way as to create populations of molecules in two different states where the populations of molecules are different from the populations before the irradiation, does not reasonably provide enablement for monitoring chemical reactions with any molecule having a fluorophore attached to it in any other chemical reaction.

In addition, there is no enablement for deteimining any kinetic quantity of any chemical reaction. The specification does not enable any person skilled in the art to which it pertains, or

with which it is most nearly connected, to make and use the invention commensurate in scope with these claims.

The Examiner then sets forth the Wands test for determining whether a disclosure meets the enablement requirement of 35 USC 112, first paragraph, the factors including:

(1) the quantity of experimentation necessary,

(2) the amount of direction or guidance presented,

(3) the presence or absence of working examples,

(4) the nature of the invention,

(5) the state of the prior art,

(6) the relative skill of those in the art,

(7) the predictability or unpredictability of the art and

(8) the breadth of the claims.

Applicants respectfully submit that under the Wands test the present specification satisfies the enablement requirement of 35 USC §112. Considering the level of understanding evidenced in the articles published in this field, the scope of the claims allowed in patents issued by the US Patent and Trademark Office in this field, and the broad variety of techniques to which FRET imaging has been applied, it must be concluded that the written description of the invention does enable any person ***skilled in the art*** to which it pertains ***to make and use the same***.

Although this technique is sometimes referred to as a "phenomenon", FRET imaging has been extensively studied and has developed into a very advanced research tool for eludidating spatio-temporal distributions and functional states of cellular constituent molecules. A review of the state of the art, including a photophysical primer, a table of methods of determining FRET in fluorescence microscopy, and a catalog of FRET microscopy methods, can be found in Jares-Erijman and Jovin "FRET Imaging", Nature Biotechnology, Vol. 21, Number 11, November 2003 (attached and available online at http://ww2.jhu.edu/csl/academics/580427/rsc/580427_6_fretreview_032106.pdf.

The mechanism of FRET ON and FRET OFF is explained – and illustrated in color – in the article by Lee et al, Ion-induced FRET On-Off in fluorescent calix[4]arene, J. Org. Chem. 2007 May 25;72(11):4242-5, and Epub 2007 May 1 at http://duongtuanquang.googlepages.com/quang-minheelee.pdf

Finally, another article co-authored by the first named author of the main reference cited by the Examiner and the first named author of the above "FRET Imaging" article is Giordano et al " Synthesis of indole-containing diheteroarylethenes. New probes for photochromic FRET (pcFRET) ARKIVOC 2005 (xii) 268-281, available on line at

http://www.arkat-usa.org/get-file/19615/

In addition to the evidence of the high level of understanding and advancement demonstrated by the above articles, Applicants refer the Examiner to patents issued by the USPTO showing the acceptance of this science, from which one must conclude that it is not necessary for the present specification to teach the basic science, but instead to teach, and claim, the advance made by the present inventors over the state of the art.

As evidence of the wide ranging practical applications of FRET techniques, and as evidence that claims of the present type have been found acceptable by the USPTO, Applicants submit for review the main claims of the following patents (and particularly US7029868 for claims including on/off; US6455268 for claiming linking group thus rebutting the Examiner's position that the specification is enabling only for monitoring chemical reactions in which the chemical species are fluorophores themselves and not for a molecule having a fluorophore attached to it; US7056683 for referring in the claim to the level of FRET):

US6291201: Fluorescence energy transfer substrates

1. A peptide Fluorescence Resonance Energy Transfer (FRET) substrate for identifying proteolytic cleavage within said peptide ....

US6248518: Method for detecting point mutations in DNA utilizing fluorescence energy transfer

1. A method for detecting point mutations in a selected target DNA sequence, ..., the method comprising:

- providing a probe having a sequence complementary to the target DNA sequence; ......

- recording an attached value of the FRET emissions from the dyes of the probe/DNA duplex;
- heating the probe/DNA duplex;
- monitoring the temperature at which the FRET emissions from the probe and duplex are reduced to a detached value as a result of the change in the proximity of the dyes to each other; and
- determining an observed melting point of the probe/target DNA duplex by recording the temperature of the probe/DNA duplex at the midpoint between the attached value of the FRET emissions and the detached value of the FRET emissions;
- whereby if the observed melting point is lower than the reference melting point at least one point mutation exists.

US6448015: Probe for detecting point mutations in DNA utilizing fluorescence energy transfer

1. A probe for detecting a point mutation in a selected target DNA sequence, the probe comprising:

- a nucleotide oligomer; and
- a pair of dyes attached to the oligomer;
- whereby the dyes act together as a donor/acceptor pair for FRET to produce an observable event when the distance between the dyes changes in response to a temperature change.

US6544746: Rapid and sensitive proximity-based assay for the detection and quantification of DNA binding proteins

1. A method of determining the activity of a DNA binding factor in a sample comprising combining two double stranded nucleic acid components with the sample wherein

- (a) each nucleic acid component comprises a portion of a DNA binding element wherein the combination of both nucleic acid components comprises a complete DNA binding element,
- (b) one nucleic acid component is labeled with a fluorescence donor and the other nucleic acid component is labeled with a fluorescence acceptor, and
- (c) the binding of a DNA binding factor or factors contained within the sample to the DNA binding element is detected by a proximity-based luminescence detection.

US6713262: Methods and compositions for high throughput identification of protein/nucleic acid binding pairs

1. A method of identifying protein/nucleic acid binding pairs, said method comprising:

- (a) contacting a molecular beacon array comprising a plurality of distinct molecular beacon probes with a population of target nucleic acids to produce a hybridized molecular beacon array, wherein each distinct probe of said plurality comprises a different probe sequence and all of said probes of said plurality share a common first fluorescent label;
- (b) contacting said hybridized molecular beacon array with a population of fluorescently labeled proteins to produce a protein bound array, where each member of said population of fluorescently labeled proteins is labeled with a second fluorescent label that makes up a FRET pair with said first fluorescent label; and
- (c) detecting any FRET generated signals from said array to identify protein/nucleic acid binding pairs on said array.

US6455268: Hydrolytic enzyme substrates and assay method

1. A compound of the formula D--L--A*, wherein D comprises a fluorescent donor moiety capable of providing a fluorescent signal, and capable of acting as a donor moiety in a FRET signal; L comprises a linking group capable of maintaining D and A in a spatial relationship suitable for FRET, and A* comprises a pre-fluorescent moiety, comprising a fluorescent moiety capable of acting as a FRET acceptor coupled to a labile group that prevents A* from providing an effective signal.

US6689574: Assays for nuclear receptor agonists and antagonists using fluorescence resonance energy transfer

1. A method of identifying an agonist of a nuclear receptor that comprises providing:

- (a) a nuclear receptor or ligand binding domain thereof labeled with a first fluorescent reagent;
- (b) CBP, p300, or other nuclear receptor co-activator, or a binding portion thereof, labeled with a second fluorescent reagent; and

...

- (d) measuring fluorescence resonance energy transfer (FRET) between the first and second fluorescent reagents;

- where the occurrence of FRET indicates that the substance is an agonist of the nuclear receptor.

US7074598: Detection of vancomycin-resistant enterococcus spp.

1. A method for detecting the presence or absence of vancomycin-resistant *enterococci* in a biological sample from an individual, said method comprising:

performing at least one cycling step, ... wherein a first vanA probe of said pair of vanA probes is labeled with a donor fluorescent moiety and wherein a second vanA probe of said pair of vanA probes is labeled with a corresponding acceptor fluorescent moiety; and

detecting the presence or absence of fluorescence resonance energy transfer (FRET) between said donor fluorescent moiety of said first vanA probe and said acceptor fluorescent moiety of said second vanA probe,

wherein the presence of FRET is indicative of the presence of vancomycin-resistant *enterococci* in said biological sample, and wherein the absence of FRET is indicative of the absence of vancomycin-resistant *enterococci* in said biological sample.

US6596499: Membrane molecule indicator compositions and methods

1. A phosphatidylinositol 4,5-bisphosphate (PIP2) indicator, said indicator comprising:

- (a) a first polypeptide comprising:
    - (i) a pleckstrin homology (PH) domain; and
    - (ii) a donor fluorescent domain
- (b) a second polypeptide comprising:
    - (i) a pleckstrin homology (PH) domain; and
    - (ii) an acceptor fluorescent domain;
        - wherein fluorescence resonance energy transfer (FRET) between said donor domain and said acceptor domain indicates PIP2 levels.

US6958210: Detection of herpes simplex virus

1. A method for detecting the presence or absence of HSV in a biological sample from an individual, said method comprising:

detecting the presence or absence of fluorescence resonance energy transfer (FRET) between said donor fluorescent moiety of said first HSV DNA polymerase probe and said acceptor fluorescent moiety of said second HSV DNA polymerase probe,

wherein the presence of FRET is indicative of the presence of HSV in said biological sample, and wherein the absence of FRET is indicative of the absence of HSV in said biological sample; ...

US6960436: Quantitative methylation detection in DNA samples

1. A method for the cytosine methylation detection in a DNA sample, comprising the following steps:

a) a genomic DNA sample is treated in a manner capable of distinguishing methylated from unmethylated cytosine bases;

b) the pre-treated DNA is amplified using at least one oligonucleotide primer, a polymerase and a set of nucleotides of which at least one is marked with a first type of label;

c) a sequence-specific oligonucleotide or oligomer probe is hybridized to the amplification product and a fluorescence resonance energy transfer (FRET) occurs if the oligonucleotide or oligomer probe, marked with a second type of label, binds in close proximity to one of the labeled nucleotides that was incorporated into the amplification product;

d) the level of methylation of the sample is determined by the level of interaction between said first and second type of label.

US7056683: Genetically encoded fluorescent reporters of kinase, methyltransferase, and acetyl-transferase activities

1. A method of determining the level of histone covalent modification in a biological sample comprising:

contacting a biological sample with a fusion protein reporter comprising a core comprising a histone-modification-specific binding domain conjugated to a histone polypeptide, wherein the core is flanked by donor and acceptor fluorescent moieties, and

monitoring the level of fluorescence resonance energy transfer (FRET) between the donor and acceptor fluorescent moieties as a result of contact with the biological sample,

wherein the level of FRET is a measure of the level of histone covalent modification in the biological sample, and

wherein the histone covalent modification is acetylation, methylation or phosphorylation.

US6472156: Homogeneous multiplex hybridization analysis by color and Tm

1. A method for analyzing a nucleic acid sample comprising three or more loci each having at least two different allelic sequences, said method comprising:

- (a) combining at least a first, a second and a third pair of oligonucleotide probes with said nucleic acid, each of the members of said pairs being capable of hybridizing in proximity to each other to a segment of said nucleic acid comprising at least one of said three or more loci, wherein (i) the first member of each pair comprises a FRET donor and the second member comprises a FRET acceptor, wherein the FRET acceptor of the second member in said first pair has an emission spectrum which is different from the emission spectrum of the FRET acceptor of said second and third oligonucleotide probe pairs, (ii) when said second and third probe pairs have the same FRET acceptor, each of said second and third probe pairs has a different Tm from each other for each different allele within the nucleic acid segment to which each member hybridizes (iii) upon hybridization, the proximity of the members of a probe pair is sufficient to allow fluorescence resonance energy transfer between said FRET donor and said FRET acceptor, and (iv) at least one of said members of each pair has a sequence which results in the differential hybridization of that member with at least two different alleles which may be present at said loci;
- (b) measuring the emission of each of said FRET acceptors at a first temperature; and
- (c) repeating said emission measurements at a second temperature; wherein the emission of said FRET acceptors at different temperatures provides an indication of the alleles present at said three or more loci.

US7425430: Probe for visualizing phosphorylation/dephosphorylation of protein and method of detecting and quantifying phosphorylation/dephosphorylation of protein

1. A probe for imaging protein phosphorylation and dephosphorylation, which comprises:

... wherein:

(i) the peptide substrate domain and the phosphorylation recognition domain are bound together by the peptide linker sequence and interposed between a donor chromophore and an acceptor chromophore that cause fluorescence resonance energy transfer (FRET) to occur; and

(ii) the peptide substrate domain, the linker sequence and the phosphorylation recognition domain are linked in order from N-terminal to C-terminal of the probe.

US7273700: Nucleic acid probe and novel method of assaying nucleic acid using the same

1. A nucleic acid probe for determining one or more types of target nucleic acids, comprising a single-stranded nucleic acid being labeled with plural fluorescent dyes, the fluorescent dyes comprising at least one pair of fluorescent dyes to induce fluorescence resonance energy transfer (FRET), the pair of fluorescent dyes comprising a fluorescent dye (a donor dye) capable of serving as a donor dye and a fluorescent dye (an acceptor dye) capable of serving as an acceptor dye, ...

US7354735: Nucleic acid encoding fluorescent protein constructs and methods for detecting apoptosis

1. An isolated nucleic acid encoding a recombinant *Aequorea victoria* fluorescent protein that detects apoptosis, said fluorescent protein comprising:

a) a donor fluorescent protein;

b) an acceptor fluorescent protein;

c) a peptide linker connecting said donor fluorescent protein to said acceptor fluorescent protein, wherein said peptide linker contains a cleavage site of a caspase, said peptide linker comprises SEQ ID NO: 23, and said cleavage site is flanked on each side with at least one glycine pair wherein XXXX represents a sequence selected from the group consisting of SEQ ID NO: 12, SEQ ID NO: 13, SEQ ID NO: 14, SEQ ID NO: 15, SEQ ID NO: 16, SEQ ID NO: 17; SEQ ID NO: 18, and SEQ ID NO: 19.

US6528275: Substrates and inhibitors of proteolytic enzymes

1. A method for screening for proteolytic activity of an enzyme applied to wells of a wellplate on one or more compounds of FRET compound mixtures applied to the wells, wherein the FRET compound mixtures define a complementary pair of compound libraries wherein the activity is the interaction of proteolytic enzyme applied to a well with one or more compounds of a mixture in the well, wherein the interaction represents cleavage of the compound by the enzyme, using a complementary pair of compound libraries L1 and L2 which constitute a set containing combinatorial fluorescence resonance energy transfer (FRET) compounds.

US7029868: Cell fusion assays using fluorescence resonance energy transfer

1. A method for determining fusion between two cell types via the measurement of fluorescence resonance energy transfer (FRET) comprising:

(a) providing a first cell that expresses β-lactamase;

(b) providing a second cell that does not express β-lactamase but contains a fluorescent substrate of β-lactamase where the substrate is a compound comprising two fluorescent moieties that are connected by a linker that is susceptible to cleavage by β-lactamase where the emission spectrum

of one moiety overlaps the absorption spectrum of the other moiety and where FRET can occur when the linker is intact but does not occur when the linker has been cleaved;

(c) measuring the amount of FRET from the substrate in the second cell in the absence of fusion between the first and second cells;

(d) bringing the first and second cells into contact under conditions such that fusion occurs; and

(e) measuring the amount of FRET from the substrate after fusion has occurred;

where the ratio of the amount of FRET measured in step (e) to the amount of FRET measured in step (c) represents the amount of fusion that has occurred, with smaller ratios indicating greater amounts of fusion.

US6730478: Method of monitoring the temperature of a biochemical reaction

2. A method of monitoring the temperature of a biochemical reaction in a reaction mixture, ...

wherein the fluorescent label utilises fluorescence transfer (FRET) as the basis of the signal ....

An see also:

US7202050: Methods for measuring phosphatase activity

US7241566: Methods and oligonucleotides for the detection of *Salmonella* sp., *E. coli* O157:H7, and *Listeria monocytogenes*

US7279317: Modulation of COP9 signalsome isopeptidase activity

US7332277: Methods for detection of genetic disorders

US7078165: Method for modulating Nod1 activity, use of a MTP related molecule for modulating Nod1 activity, and therapeutic applications thereof

US6872525: Method for selectively separating live cells expressing a specific gene

US6897031: Multiparameter FACS assays to detect alterations in exocytosis

US6630311: Fluorescence-based high throughput screening assays for protein kinases and phosphatases

US6456734: Calibration of fluorescence resonance energy transfer in microscopy

US7449151: Fluorescence resonance energy transfer analyzer

It is the task of the present written description of the invention to enable any person ***skilled in the art*** to which it pertains ***to make and use the same.***

As can be seen from the above, the level of skill in the art is high, and, given the familiarity acquired over a decade of continuous development and publication, it can not be said that the level of unpredictability is so high that all possible variables must be tested.

In order to understand whether the present invention is adequately described, it must first be determined what the present invention is in comparison with the state of the art.

As explained in paragraph [0004] – [0006], classical methods of relaxation kinetics are well known, but the intensive thermodynamic quantity has to be varied, which represents a potential strain on the chemical species, and delicate biological material (e.g., living cells) may easily be damaged.

Paragraph [0007] explains that fluorescence resonance energy transfer, FRET, is known, imaging FRET techniques in a microscope as well as non-imaging techniques are known, e.g. in structural analysis of biological molecules or in DNA hybridisation experiments. FRET is also used in rapid assays, and in detecting certain molecules. Switchable FRET-acceptors are discussed in paragrah [0008].

As discussed in paragraph [0009], Taking into account the well known methods of relaxation kinetics, it is the object of the invention to further develop ***a generic method*** such that measurements of relaxation kinetics ***with reduced strain on the species*** involved in the reaction become possible.

As explained in paragraph [0011], this invention is based on an ***inversion of the principles of application of conventional measurements of relaxation kinetics***. As explained, in conventional methods the position of equilibrium of a reaction is changed by a variation of an intensive thermodynamic quantity and the relaxation of concentrations into the new equilibrium state is observed. However, with the present invention the relative concentrations of the species involved are suddenly changed (by switching the photochromic FRET acceptor from its first

photochromic state into its second photochromic state) and their return into the (thermodynamically unchanged) equilibrium state is observed.

Besides the advantage of a very gentle displacement of concentrations the method according to the invention has, in comparison to conventional relaxation methods, the further advantage to be technically particularly easy to implement since all that is needed to establish the non-equilibrium state is a controllable light source. Due to the easiness of its setup the method is also suited for use in portable devices for fast in-situ measurement, e.g. when searching particular chemical substances affecting the kinetics of a reaction.

This switching process affects the species including the FRET acceptor both as a free ligand as well as in its bound state. The non-equilibrium state is generated because in the bound state a FRET channel of de-excitation is available which is not available for the free ligand as will be explained in greater detail below. Thus, at the end of the switching process the bound state portion with its FRET acceptor in the altered photochromic state is too small compared to the free ligand. The return of the system into its equilibrium state may be observed in several ways by time-resolved fluorescence measurements, since the photochromic states in the bound state may be differentiated from each other due to their different FRET efficiencies.

Accordingly, those familiar with the principles of conventional measurements of relaxation techniques, given the insight of the present invention, will be able to understand how to carry out the present invention wherein light is used for generating a non-equilibrium state.

35 U.S.C. 112, second paragraph

Claims 1-13 are rejected under 35 U.S.C. 112, second paragraph, as being indefinite for failing to particularly point out and distinctly claim the subject matter which applicant regards as the invention.

Claims 1-13 are indefinite in claim 1. Claim 1 is indefinite over the recitation of "relaxation of concentrations". It is not clear what is meant by this term.

In response, Applicants refer the Examiner to paragraph [0017] of the specification, teaching "Thus, a relaxation of concentrations is established, which does not match the

thermodynamic position of equilibrium. Starting from this non-equilibrium state, ***a balancing of concentrations, i.e. a relaxation, occurs*** having--in this case--a relaxation time of $\tau=1/(k_f[D]+k_r)$, which is well known from the classical methods of relaxation. In a more complex reaction a multiexponential behaviour is to be expected which also is related to the rate constants involved via known equations. The process of relaxation may be observed through the fluorescence of at least one of the fluorophores involved."

Accordingly, withdrawal of the rejection is respectfully requested.

<u>Claim Rejections - 35 USC § 102</u>

Claims 1-3 and 7-13 are rejected under 35 U.S.C. 102(b) as being anticipated by Giordano et al. (J. Am.Chem. Soc., vol 124, pp 7481-7489, 2002; cited in the IDS) as evidenced by the Supplemental material (J. Am. Chem. Soc., vol. 124, 2002).

Regarding claim 1, Giordano et al. teach a method of determinic characteristic kinetic quantity of a chemical reaction reaction in a sample involving a plurality of chemical species, at least one of said species including at least one fluorophore (Fig. 1; page 7482, last paragraph; page 7483, first paragraph; Table 1; page 7485, second paragraph; page 7486, paragraphs 1-3), the method comprising the steps of:

generating, by impinging light on said sample, a non-equilibrium state of said chemical reaction (page 7483, paragraphs 1-4; Fig. 4), and

observing, by means of a fluorescence signal of at least one fluorophore, at least one portion of a relaxation of concentrations of said species involved (Fig. 4),

the method wherein at least one product of said chemical reaction under test comprises a combination of two species each of which including one partner of a FRET pair consisting of a FRET donor and a FRET acceptor wherein said FRET acceptor is a photochrome, the absorption spectrum of which being changeable by irradiation with light of a suitable wavelength (Fig. 1; page 7482, paragraphs 3-8);

wherein said FRET donor is a fluorophore, the emission spectrum of which having an overlap region with said FRET acceptor's absorption spectrum, the size of said overlap region

being dependent on the photochromic state of said FRET acceptor (Fig. 1; page 7482, 7th paragraph);

and wherein said light used for generating said non-equilibrium state has a wavelength capable of switching said photochromic state of said FRET acceptor (Fig. 1; page 7482, paragraphs 5-8).

Applicants respectfully traverse.

Giordano et al do not teach generating, by impinging light on said sample, a non-equilibrium state of said chemical reaction, and observing, by means of a fluorescence signal of at least one fluorophore, at least one portion of a relaxation of concentrations of said species involved.

Giordano et al merely teach that several molecules from the family of diheteroarylethenes, when irradiated by suitable light, show a reversible change in conformation between an open ring configuration and a closed ring configuration. Along with this change in structure comes a substantial change in the excitation spectrum of the molecules. Such a chromophore may be applied as a switchable FRET acceptor. If there is a suitable FRET donor, the emission spectrum of which overlaps in a strongly different way with each of the chromophore's different conformations, the FRET efficiency may be varied by irradiation with light causing the change in conformation. The molecules disclosed in said document may optionally be switched between two photochromic states by irradiation with light of different wavelengths, in particular UV light and visible light. Slangily spoken, one can speak of switching FRET on and off wherein the ON state corresponds to a larger overlap region of the FRET donor's emission spectrum with the FRET acceptor's excitation spectrum--thus, a higher FRET efficiency--and wherein the OFF state corresponds to a smaller overlap region--thus, a lower FRET efficiency. Although usually photochromic molecules are not fluorescent, some photochromic fluorophores are known.

As explained in paragraph [0011], the present invention is based on an ***inversion of the principles of application of conventional measurements of relaxation kinetics***. As explained, in conventional methods the position of equilibrium of a reaction is changed by a variation of an

intensive thermodynamic quantity and the relaxation of concentrations into the new equilibrium state is observed. However, with the present invention the relative concentrations of the species involved are suddenly changed (by switching the photochromic FRET acceptor from its first photochromic state into its second photochromic state) and their return into the (thermodynamically unchanged) equilibrium state is observed.

Besides the advantage of a very gentle displacement of concentrations the method according to the invention has, in comparison to conventional relaxation methods, the further advantage to be technically particularly easy to implement since all that is needed to establish the non-equilibrium state is a controllable light source. Due to the easiness of its setup the method is also suited for use in portable devices for fast in-situ measurement, e.g. when searching particular chemical substances affecting the kinetics of a reaction.

Regarding claim 2, Giordano et al. teach detecting the fluorescence of the donor (Fig. 2). Regarding claim 3, Giordano et al. teach detection of the fluorescence of the acceptor (Fig. 3, 4).

Regarding claim 7, Giordano et al. teach the first and second directions of the reaction excited by two different wavelengths (Fig. 1; Table 1).

Regarding claim 8, Giordano et al. teach UV light (Fig. 1; Table 1).

Regarding claims 9 and 10, Giordano et al. teach irradiation with visible light (Fig. 1; Table 1).

Regarding claim 11, Giordano et al. teach that the intensity of irradiation used for photoconversion is higher than the intensity of irradiation used for fluorescence measurement (Supplemental material page 5, last paragraph; page 6, first and second paragraphs).

Regarding claims 12 and 13, Giordano et al. teach irradiating the sample in a temporally modulated fashion using two different wavelengths (Fig. 6).

Applicants submit that these claims are patentable by virtue of their dependency from claim 1, the patentability of having been explained above.

Accordingly, withdrawal of the rejection is respectfully requested.

Claim Rejections - 35 USC § 103

Claims 4-6 are rejected under 35 U.S.C. 103(a) as being unpatentable over Giordano et al. Giordano et al. teach a system with one acceptor and one donor, but do not teach a system with an additional acceptor.

Regarding claims 4-6, Watrob et al. teach using a system with one donor and two acceptors (Scheme 1; page 7337, 7338).

It would have been prima facie obvious to one of ordinary skill in the art at the time of the invention to have used additional acceptor of Watrob et al. in the method of Giordano et al. The motivation to do so is provided by Watrob et al., who state (page 7342, last paragraph):

"Three-chromophore FRET systems offer several advantages. First, three-chromophore systems report the simultaneous proximity of three species and provide the ability to measure two or three distances in a complex. Structural information about the assembly can then be inferred from the relative positions of individual components of the complex. For example, in Case I where no FRET1 -> 3 occurs, r13 must be >1.5 R013. This restricts the position of 3 relative to 1 to a minimal distance of r13 — 1.75 Ron and a maximal distance of r13 = r12 + r23 for a linear arrangement of 1, 2, and 3. Second, in the case of linear or near linear arrangement of the three chromophores, two-step FRET extends the distance range for detection of simultaneous proximity. For example, assuming

Ro = 55 A for the two FRET pairs and a detection limit of 1.5 Ro, one-step FRET at a distance r = 83 A has an efficiency Eij = 0.08. A two-step FRET relay with Erelay = 0.08 corresponds to a total distance r = 127 A. Thus, the detectable distance range increases by as much as 50%. Third, threechromophore systems require fewer labeled samples to measure two or three distances than conventional one-step FRET."

In response, Applicants submit that these claims are allowable by virtue of their dependency from allowable claim 1.

Accordingly, withdrawal of the rejection is respectfully requested.

The Commissioner is hereby authorized to charge any fees which may be required at any time during the prosecution of this application without specific authorization, or credit any overpayment, to Deposit Account Number 16-0877.

Favorable consideration and early issuance of the Notice of Allowance are respectfully requested. **Should further issues remain prior to allowance, the Examiner is respectfully requested to contact the undersigned at the indicated telephone number.**

Respectfully submitted,

Stephan A. Pendorf
Registration No. 32,665

Patent Central LLC
1401 Hollywood Blvd.
Hollywood, FL 33020-5237
(954) 922-7315

Date: January 6, 2009

nature biotechnology

FRET imaging

Elizabeth A Jares-Erijman[1] & Thomas M Jovin[2]

Förster (or Fluorescence) Resonance Energy Transfer (FRET) is unique in generating fluorescence signals sensitive to molecular conformation, association, and separation in the 1–10 nm range. We introduce a revised photophysical framework for the phenomenon and provide a systematic catalog of FRET techniques adapted to imaging systems, including new approaches proposed as suitable prospects for implementation. Applications extending from a single molecule to live cells will benefit from multidimensional microscopy techniques, particularly those adapted for optical sectioning and incorporating new algorithms for resolving the component contributions to images of complex molecular systems.

Biological phenomena are based on the fundamental physico-chemical processes of molecular binding, association, conformational change, diffusion and catalysis. The structural hierarchy established at the level of organelles, cells, tissues and organisms is imposed via an extensive network of cascade and feedback mechanisms based on these reactions. Thus, in order to perform 'biochemistry in the cell' it is imperative to elucidate the spatio-temporal distributions and functional states of the constituent molecules. Fluorescence microscopy is ideally suited to this task because it generates contrast by exploiting the many manifestations of light emission: sensitivity, selectivity, and modulation via reactions in the ground and excited electronic states. Of these, FRET (for a discussion of nomenclature, see Table 1.1 in ref. 1) is unique in providing signals sensitive to intra- and intermolecular distances in the 1–10 nm range. Thus, FRET is capable of resolving molecular interactions and conformations with a spatial resolution far exceeding the inherent diffraction limit (~λ/2) of conventional optical microscopy, yet is also compatible with super-resolution techniques.

This report is intended primarily as a guide to FRET in the imaging environment, although most of the concepts are applicable to solution studies as well. Space limitations preclude a survey of applications, for which the reader is referred to recent reports and reviews[2–11]. We present a somewhat revised formalism for the FRET phenomenon that offers certain advantages over standard analyses and provide a systematic classification of 22 different FRET methods (see also ref. 11). These include several new approaches of potential utility in the research and biotechnological laboratories. We conclude with a brief discussion of selected probe issues and anticipated future developments extending from single molecule to live cell applications.

Fluorescence resonance energy transfer

FRET is a process in which energy is transferred nonradiatively (that is, via long-range dipole-dipole coupling) from a fluorophore in an electronic excited state serving as a donor, to another chromophore or acceptor. The latter may, but need not, be fluorescent. Recent monographs[1,9,10,12,13] and two reviews by R. Clegg[14,15] provide excellent and extensive coverage of this topic.

The transfer rate k_t (see **Box 1** for definitions and basics) varies inversely with the 6th power of the donor-acceptor separation (r^6) over the range of 1–10 nm, as first demonstrated with peptides 40 years ago[16]. Such distances are relevant for most biomolecules or their constituent domains engaged in complex formation and conformational transition. The transfer rate also depends on three parameters: (i) the overlap of the donor emission and acceptor absorption spectra (parameter: overlap integral J); (ii) the relative-orientation of the donor absorption and acceptor transitions moments (parameter: κ^2, range 0–4); and (iii) the refractive index (parameter: n^{-4}, range ≅ 1/3–1/5).

The quantitative treatment of FRET originated with Theodor Förster and is embodied in widely disseminated formulas for k_t, the 'Förster constant' R_o, and the transfer quantum yield generally denoted as the energy transfer efficiency E (equation (1)).

$$k_t = \frac{1}{\tau_o}(R_o/r)^6;\ R_o^6 = c_o\kappa^2 J n^{-4} Q_o = c_o\kappa^2 J n^{-4}(k_f\tau_o);\ E = k_t\tau = \frac{(R_o/r)^6}{1+(R_o/r)^6};$$
$$\tau_o^{-1} = k_f + k_{nr} + k_{isc} + k_{pb};\ \tau^{-1} = \tau_o^{-1} + k_t \qquad (1)$$

where $c_o = 8.8 \times 10^{-28}$ for R_o in nm and $J = 10^{17}\int q_{d,\lambda}\,\varepsilon_{a,\lambda}\lambda^4 d\lambda$ in nm^6 mol^{-1}; $q_{d,\lambda}$ is the normalized donor emission spectrum. As shown in equation (1), the unperturbed lifetime of the donor, τ_o, appears both in the denominator and in the numerator (second expression for R_o^6). Thus, upon canceling terms one is left only with the radiative rate constant k_f in the numerator. This quantity reflects inherent properties of the fluorophore, including solvation, and can generally be regarded as invariant under given experimental conditions[13,17]. It follows that the fundamental relationship established by Förster between k_t and k_f bears no necessary relationship to the reference donor lifetime τ_o or to the derived quantum yield Q_o. That is, the inclusion of these quantities in the definition of R_o is arbitrary, and justified only because most, but not all, estimations of the transfer efficiency (E) are made by comparisons with the properties of the unperturbed donor. (It is interesting that in his widely cited English review[18], Förster made no mention of R_o,

[1]Departamento de Química Orgánica, Facultad de Ciencias Exactas y Naturales, Universidad de Buenos Aires, 1428 Buenos Aires, Argentina. [2]Department of Molecular Biology, Max Planck Institute for Biophysical Chemistry, 37077 Göttingen, Germany. Correspondence should be addressed to E.A.J.-E. (eli@qo.fcen.uba.ar) or T.M.J. (tjovin@gwdg.de).

Published online 31 October 2002; doi:10.1038/nbt896

although he commented on the remarkable absence of Planck's constant from $n_{a \to b}$, his expression for k_t.)

A major problem with cell biological applications of FRET, particularly those involving imaging techniques, is that the reference value τ_o is generally unknown and may vary continuously and arbitrarily throughout the sample, for example as a result of changes in the generally environment-sensitive k_{nr}. In addition, although the donor-separation distance r is of primary interest in most FRET experiments, one or more of the other parameters incorporated in the definition of R_o may also change or be of even greater functional significance. Possible examples would be molecular translocations between the cytoplasm and the plasma membrane, and conformational rearrangements. Of central relevance in the latter instance is the orientational factor, κ^2, to which one almost universally assigns the value of 2/3. Unfortunately, this procedure is valid only if the donor and acceptor molecules are oriented randomly and rotate rapidly and isotropically during the donor excited-state lifetime. Such a condition may often or generally fail to exist, as with the visible fluorescent proteins (VFPs), the rotational correlation times (see below) of which are ~fivefold their lifetimes, thereby greatly limiting the extent of rotational relaxation[19,20]. (It follows that R_os reported for the various VFPs (ref. 21) must be used with caution.) For a random yet static molecular distribution, the ensemble κ^2 is not even a constant but

Table 1 Methods for determining FRET in fluorescence microscopy

Category	Method	Resonance energy transfer parameters	References
I. Donor quenching and/or acceptor sensitization			
Ia. Combined donor (D) and acceptor (A) emission signals			
Ia1	2,3 signals; spectra	Calibrated functions	3,11,14,15,36,50,66–69
Ia2	Normalized D/A ratio	$\theta = Q_a R_{da}$; $R_{da} \propto I^{d}_{da,d}/I^{a}_{da,d}$	67,70
Ia3	Bioluminescence RET (BRET)	$\theta \propto I_b/I_a$	71
Ib. Fluorescence-detected excited state lifetime(s) (FLIM)			
Ib1	D lifetime	$\rho = \tau/\tau_o$	2,9,17,31,63,72–83
Ib2	Luminescence RET (LRET)	$\rho = \tau^{a}_{da,d}/\tau_o$	70
Ib3	Combined D,A lifetimes	Frequency domain: τ_ϕ, τ_m correlations	20,75
Ib4	Spectral FLIM (sFLIM)	D and A lifetimes as functions of λ_{exc}, λ_{em}	77,79,81
Ic. Donor intensity and intensity ratios			
Ic1	Intensity	$\rho = I/I_o$	
Ic2	On-off ratio	$\rho = \mathrm{OnOff}_o/\mathrm{OnOff}$	Proposed
Ic3	Excited state saturation	$\rho = \zeta/\zeta_o$; $\zeta = \frac{\Psi_2/\Psi_1 - I_2/I_1}{I_2/I_1 - 1}$	Proposed
Ic4	Ground state depletion (triplet)	$\theta = \left(\frac{1}{\sigma\tau_T\Psi}\right)\left(\frac{Q_f}{Q_{isc}}\right)\frac{(1-\varphi)(1-\varphi_o)}{\varphi - \varphi_o}$; $\varphi = \frac{I_{long}}{I_{short}}$	Proposed
Id. Donor depletion kinetics			
Id1	D pb kinetics (pbFRET)	$\rho = \tau_{pb,o}/\tau_{pb}$	25,26,84,85
Id2	Integrated D pb	$\rho = \zeta/\zeta_o$; $\zeta = I(t=0)/\int_0^\infty I(t)dt$	25,84
Id3	Intersystem crossing	$\rho = \tau_{isc,o}/\tau_{isc}$	Proposed
Ie. Acceptor depletion (adFRET)			
Ie1	Direct A pb (irreversible)	Combination with Ib1–2, Ic1–4, Id1–3, IIa1	26,86,87
Ie2	Photochromic A (pcFRET)	Combinations as in Ie1; example (with Ic1): $\rho = 1 - \frac{1 - I_{on}/I_{off}}{\alpha_{on} - \alpha_{off}(I_{on}/I_{off})}$	27,28
Ie3	A saturation (frustrated FRET)	Combinations as in Ie1; example (with Ic1): $\rho = \alpha_{sat}(I_{\alpha_{sat}}/I + \alpha_{sat} - 1)^{-1}$	Proposed
Ie4	Sensitized A pb kinetics (PES)	$\rho = 1 - \frac{\sigma_a}{\sigma_d}\left(\frac{\tau_{pb,o}}{\tau_{pb}} - 1\right)$	30
II. Emission anisotropy			
IIa. Steady-state anisotropy			
IIa1	Donor anisotropy $\bar{r}$	$\rho = \zeta/\zeta_o$; $\zeta = \left(\frac{r_o - \bar{r}}{\bar{r} - r_\infty}\right)$	10,12,88
IIa2	Acceptor anisotropy $\bar{r}$	$\rho = 1 - \frac{\sigma_a}{\sigma_d}\left(\frac{\bar{r}_o}{\bar{r}} - 1\right)$	Proposed
IIb. Homotransfer, energy migration FRET (emFRET, P-FRET)			
IIb1	Steady-state anisotropy $\bar{r}$	$\bar{r} = \frac{r_o(1 - \gamma e^{\gamma^2}\pi^{1/2} erfc[\gamma])}{1 + \tau/\phi}$; $\gamma = \left(\frac{Q_o}{1 + \tau/\phi}\right)^{1/2}\frac{\Gamma_o^3 c}{750}$	1,9,12,31,32,64,88–90
IIb2	Dynamic r (rFLIM, P-FRET)	Functions of r_o, r_∞, ϕ, τ	9,20,31,63,72,83,91

Subscripts refer either to species composition, excitation or photophysical process; a subscript 'o' refers to a reference state of either D (assumed unless otherwise indicated) or A, in which the other component is absent. Superscripts indicate whether emission is measured in the D or A spectral regions and assumes correction for spectral crosstalk (for example, D→A). See equations (1–4) for definition of terms and symbols (σ, Ψ, Q, θ, ρ). I, signal intensity; (Ia3) I_b, bioluminescence signal; (Ic4) I_{long} and I_{short}, signals at end and beginning, respectively, of a given exposure time. In some cases, the need for calibration (scaling) factors is indicated by the symbol '$\propto$'; (Ie2) α_{on}, fractional transition to the FRET-competent photochromic form of the A upon UV irradiation, and α_{off}, fractional transition to the FRET-incompetent photochromic form of the A upon visible irradiation; (Ie3) α_{sat}, degree of light-induced formation of the FRET-incompetent excited state of the A; $I_{\alpha_{sat}}$, D intensity corresponding to α_{sat}; (IIb1) see text for definitions; c in mM units.

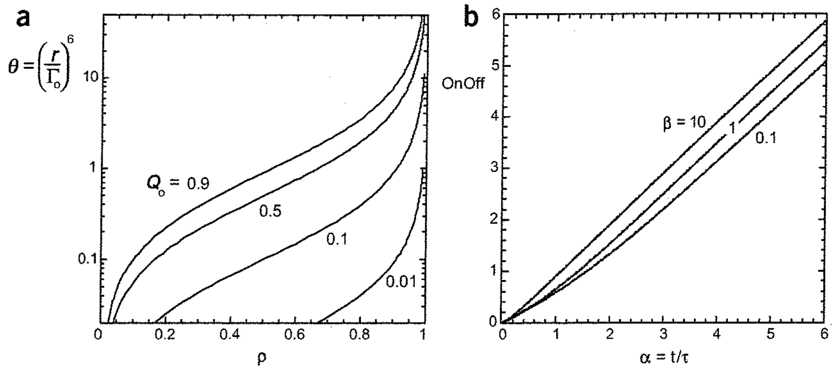

Figure 1 Parametric FRET functions. (**a**) Förster factor θ as a function of a ratio function ρ. The latter involves combinations of parameters or functions equivalent to the ratio of the FRET-quenched and unquenched donor quantum yields, (equation (4) and **Table 1**). Operation in the linear irradiance regime (**Fig. 2**) is assumed. (**b**) FRET technique based on OnOff ratio (equation (4) in **Box 1**), which directly yields the fluorescence lifetime (via α) for any degree of saturation (β).

instead a function of the donor-acceptor separation r.

A further issue is the donor-acceptor stoichiometry. In the case of a donor surrounded by n equivalent acceptors, the operational R_o^6 is ~n times that for the single donor–acceptor pair, and for point-to-plane transfer, the distance dependence varies with the 4th, and not the 6th, power of the separation[22]. In short, the concept of a 'constant' resonance energy transfer (RET) parameter, such as R_o, is not universally applicable.

In our estimation, the relationship of k_t to many of the experimental means for its determination (see **Table 1**) may be expressed more naturally by recourse to alternative formulations, and we propose the one represented in equation (2).

$$\theta \equiv \frac{k_f}{k_t} = \left(\frac{r}{\Gamma_o}\right)^6; \Gamma_o^6 = c_o\kappa^2 J n^{-4}; R_o^6 = Q_o\Gamma_o^6 \qquad (2)$$

$$\theta = Q_o\left(\frac{\rho}{1-\rho}\right); \rho = 1 - E = \frac{Q}{Q_o} \text{ or any other equivalent ratio or function.} \qquad (3)$$

We define the inverse proportionality constant between k_t and k_f as a 'Förster Factor' θ, and equate it to the 6th power of the ratio of the separation distance r and a Förster constant Γ_o in which Q_o is absent. It is important to recognize that the other parameters defining Γ_o may also vary in particular experiments, either by experimental design or nature of particular targets, or from changes in the inherent population distribution of molecular states. In the latter case, appropriate ensemble averaging formalisms must be employed[1,3,11,12–15].

We now extend the formalism further (equation (3)) by relating θ to ρ, a ratio of experimental quantities (**Table 1**) proportional to the donor quantum yields corresponding to the two conditions: donor with acceptor (presence of RET); and donor without acceptor (absence of RET). From equation (3) and **Fig. 1a**, it is seen that a reduction in donor Q_o has two consequences. First, it displaces the transition inflection point, and thus the greatest sensitivity of ρ, from θ = 1 to smaller values (smaller r). And second, it restricts the operative dynamic range of the determinations to higher values of ρ. A further consideration, already stated earlier, is that the nonradiative decay pathway and thus Q_o can also change dramatically between alternative molecular states represented in a particular FRET experiment.

A catalog of FRET microscopy methods

In devising methods for exploiting FRET in microscopy, one is faced with two fundamental challenges: first, the formalism must be appropriate for quantifying FRET under conditions of arbitrary, generally unknown, intramolecular and/or intermolecular stoichiometries, distributions and microenvironments of donor and acceptor; second, continuous methods of observation (by FRET) are desirable in most studies of live cells. Numerous other considerations dictate the choice of FRET techniques for imaging purposes and lead us to the classification scheme given in **Table 1**.

We include several new strategies (Ic2–4, Id3, Ie2–3, Ie4, and IIa2) with potential for implementation in fluorescence microscopy. The methods are assigned to two groups (I and II) depending on whether they are based on intensity and kinetic donor-acceptor relationships or on emission anisotropy. In many instances, as in the 'ρ methods' (Ib1–2, Ic1–3, Id1–3, Ie1–4, and IIa1–2), the reference measurement alluded to above (*e.g.*, donor I_o or τ_o) is required. It can be provided either by a separate region or sample, if available, or by recourse to the various acceptor depletion strategies (Ie). The determination of the Förster Factor θ by some other techniques (Ia2–3, IIb1–2) does not require Q_o as a scaling factor.

We stress the desirability of quantitative determinations by supplying equations based on the formalism introduced above. That is, we favor the view that the generation of secondary images representing FRET-related or FRET-derived parameters is the primary goal. The formulas differ as to whether they are restricted to the linear irradiance regime, and apply either to a single donor-acceptor pair or to arbitrary donor-acceptor stoichiometries and thus an ensemble of molecular species. Generalization is possible but beyond the scope of this report; for Monte Carlo simulations of some cases of **Table 1**, see ref. 11.

In the following text, we provide brief explanations of the different entries outlined in **Table 1**. Two points are worth emphasizing at the outset. First, the methods with greatest sensitivity for low transfer efficiencies—in some cases coupled with fast acquisition capability—include Ia2–3, Ib2 and Ie2–4. Second, methods differ with respect to their applicability in point-scanning as opposed to wide-field microscopes.

In well-defined (usually intramolecular) single-donor, single-acceptor systems, fluorescence ratio measurements involving different spectral components (donor and acceptor signals) can be calibrated so as to yield the FRET efficiency. These techniques (Ia1) are difficult to implement because they require acquisition and registration of multiple images,

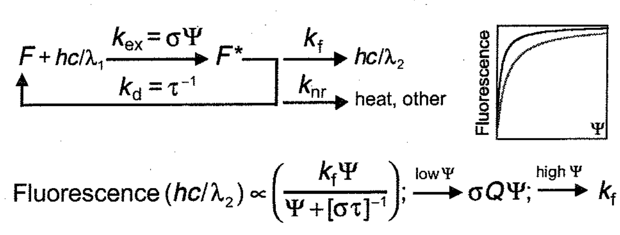

Figure 2 The 'Michaelis-Menten' view of a fluorophore as a photon conversion catalyst or 'enzyme' (see **Box 1**). The two saturation curves depicted differ in στ by a factor of 3 (lower value in red).

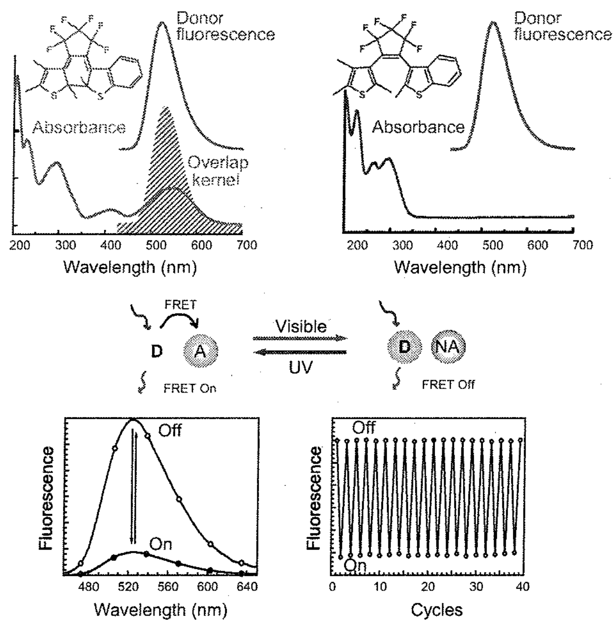

Figure 3 Photochromic FRET (pcFRET). The chemical structures depicted correspond to the photochromic dithienylethene in the colorless open form (right upper) and colored closed form (left upper). The absorption spectrum of the latter overlaps well with the emission spectrum of the donor; the kernel of the overlap integral (striped) corresponds to the lucifer yellow donor selected for a model compound[27]. Ultraviolet light induces the photochromic transition to the closed form (On), and visible (green) light reverses the process to the open form (Off). Bottom: corresponding donor spectra and multiple cycles between the two states of the system. The photophysical scheme is represented in **Figure 5c**.

correction for spectrally overlapping donor and acceptor signals and direct excitation of the acceptor, as well as due consideration of variable donor-acceptor stoichiometries in the equations used to compute ρ and θ. The ratio of the quenched donor and sensitized emission signals (Ia2) is unique in being scaled by the acceptor instead of the donor quantum yield in the calculation of θ. By employing a bioluminescent donor (Ia3)—for example, luciferase as an expressed fusion protein—excitation by light is not required, thereby suppressing autofluorescence background and photobleaching.

The direct determination of fluorescence lifetime (Ib1), either in the time or in the frequency domain, is one of the most direct measures of FRET. It is also relatively insensitive to variations in concentration and optical path length. Selection of a donor with a long lifetime and high transfer efficiency (Ib2), such as lanthanide-chelates, permit sensitive measurements of donor quenching (that is, of very low transfer efficiencies) because the (quenched) donor decay is monitored via the sensitized (shorter-lived) acceptor emission, thereby ensuring a low background. Sample/microenvironmental heterogeneity can be assessed with FRET by exploiting numerous formalisms for time- and frequency-domain measurements (Ib3), particularly if the fluorescent lifetimes can be correlated with continuous emission and/or excitation spectra via multiplexed, transform-encoded acquisition (Ib4).

FRET determinations derived from intensity relationships (Ic1) require an accurate reference for the acceptor-free donor signals and are difficult to achieve in practice except, for example, in combination with acceptor depletion schemes (Ie) or recourse to appropriately fabricated nano-microstructures. The use of 'dark' acceptors falls into this general category.

We introduce here three new approaches (Ic2–4) for the exploitation of intensity measurements by use of the photophysical principles outlined earlier and constituting indirect estimations of the fluorescence lifetime. The first (Ic2) is based on the OnOff function (see **Box 1**, equation (4)). This relationship provides a direct determination of τ for any degree of donor saturation (at saturation, the relationship is linear; see **Fig. 1b**). Implementation should be simple (*e.g.*, using a detector with swinging dual integrated outputs). A second method (Ic3) is based on the displacement to the 'right' of the singlet saturation curve due to the FRET-induced shortening of the fluorescence lifetime (**Fig. 2**). Measurements are performed at two levels of irradiance (denoted by subscripts 1,2 in **Table 1**, Ic3), one of which has to be sufficiently high (that is, above the linear range). The indicated function involving the ratios of irradiances and signals yields $\sigma\tau$. The acceptor should have a short lifetime to prevent its saturation via FRET. Distortions of the imaging point-spread-function may arise from donor saturation, particularly when using scanning systems; these effects can either reduce or enhance[23,24] spatial resolution. In wide-field systems, such problems vanish although high-energy sources are required. Finally, in Ic4 we exploit the triplet lifetime τ_T, which can be extended from the microsecond characteristic of oxygen-saturated systems to the millisecond domain (depending on the fluorophore) by oxygen depletion via argon flushing or chemical reductants. Measurements performed after short and long exposure times, defined in relation to τ_T, differ by virtue of depletion of the singlet manifold to an extent reflecting FRET-induced changes in the fluorescence lifetime.

FRET determinations based on donor depletion kinetics are also in widespread use. Donor photobleaching (Id1) occurs with a time constant that is inversely related to the donor quantum yield. Inasmuch as the process generally occurs on a timescale 6–12 orders of magnitude greater than the usual nanosecond range of fluorescence decay, the method is easy to implement. It also circumvents the registration problem of disparate images (assuming no sample movement) and the need for spectral overlap factors (as in Ic1), and does not require a fluorescent acceptor, although the latter must be photostable. Another reason accounting for the popularity of pbFRET is its good performance at low transfer efficiencies. A variant of pbFRET (Id2) introduced at the same time as Id1 (ref. 25) has not been adopted generally, despite its ideal suitability for detection with charge-coupled dipole (CCD) cameras. The underlying principle, first announced by the remarkable spectroscopist, the late Thomas Hirschfeld, is the invariance (quantum yield independence) of the total integrated emission during quantitative photobleaching of a fluorophore. The integrated image serves to normalize a corresponding initial quenched donor image of the same area. A third, new kinetic method (Id3) involves the measurement of the kinetics of ground-state depletion via intersystem crossing to the triplet state of the donor. As in Ic3, one requires conditions favoring the maintenance of a long triplet lifetime.

The methods we have combined under the designation 'acceptor depletion' FRET (adFRET; Ie) are of fundamental importance because they permit the generation '*in situ*,' that is, at every sample position, of the reference state required for many of the other techniques. Note that this category corresponds to 'T_0 (or R_0) engineering' in the sense that one perturbs the system by altering the value of J (see equation (1)).

In 1995, we implemented irreversible acceptor photobleaching (Ie1) upon noting the difficulty of performing donor pbFRET (Id1) with the very good FRET donor-acceptor pair of cyanine dyes Cy3–Cy5 (ref. 26). Cy3 is highly photostable (the newer version Cy3b even more so), whereas Cy5 photobleaches readily; it became apparent that

photobleaching the latter provided 'before' and 'after' images from which the FRET efficiency could be readily determined. This technique is used extensively due to its many virtues: (i) it is simple and rapid; (ii) only donor images are required, avoiding registration problems; (iii) there is automatic correction for pixel-by-pixel variations in the reference donor quantum yield (lifetime); (iv) it is very effective for high-transfer efficiencies ('disappearing' donor; see Figures 2 and 3 in ref. 26); (v) it works well with 'dirty,' that is, relatively impure acceptors; and (vi) it can be combined with Id1,2 (ref. 26).

Photochromic FRET (pcFRET; Ie2) is the reversible equivalent of Ie1 and thus offers the prospect of continuous measurements with cellular samples. A photochromic acceptor is cycled repeatedly between FRET 'competent (on)' and FRET 'incompetent (off)' states by alternative exposures to visible and UV light[27,28] (Fig. 3). Besides being reversible, pcFRET is superior to Ie1 in having a high quantum yield for photoconversion. That is, few absorbed photons are required to induce the interconversions between states, in contrast to $\sim 10^{4-6}$ photons for irreversible photobleaching. We are adapting pcFRET for microscopy by optimized chemical design of the photochromic probes and incorporation of modulated light sources and detectors to permit very sensitive detection, especially of low FRET efficiencies. In addition, we have devised a scheme for applying the pcFRET concept in determinations of reaction kinetics (pcRelKin, patent applied for by the authors). This relaxation technique is potentially suited for very small volumes and high speed.

Two new adFRET techniques are proposed here. In the first (Ie3), the acceptor is driven into saturation so as to 'frustrate' FRET[23,29], and thereby restore the donor emission to its unquenched level. The use of modulated light sources (of which two are required) and phase-sensitive detection (with a lock-in amplifier) should provide a very sensitive measurement, particularly in laser spot scanning systems. A photostable long-lived acceptor is required.

Another new and intriguing FRET method (Ie4), to our knowledge not yet applied in microscopy, was designed to detect extremely low FRET efficiencies in solution (the author claimed the potential for detecting an E of 10^{-4} over a distance of 20 nm[30]). This technique is based on the measurement of the photobleaching kinetics of a photolabile acceptor excited by a donor via FRET. The low background and high sensitivity are achieved by exciting the donor, preferably a fluorophore with a large Stokes shift, at a wavelength of minimal absorption by the acceptor.

Emission anisotropy, a dimensionless quantity defined in terms of the two polarized emission signals arising from polarized excitation, provides a steady-state ($\bar{r}$) or time-dependent measure of rotational diffusion and is thus sensitive to size, shape, association and motion. The parametric descriptors are the fluorescence lifetime, the rotational correlation time(s) ϕ, and the initial (r_0) and final (r_∞, limiting) anisotropies dictated by the intrinsic transition moments and molecular asymmetry, and the environmental anisotropy, respectively. The determination is based on signal ratios and thus shares with the lifetime a relative insensitivity to optical thickness, light intensity and concentration. We can identify at least two FRET methods based on fluorescence anisotropy. By virtue of the relationship between the rotational diffusion parameters, the donor $\bar{r}$ is a function of the ratio τ/ϕ[31]; thus, a change in the lifetime will be reflected in $\bar{r}$ (IIa1). We propose a second technique (IIa2) involving the selection of an excitation wavelength capable of exciting both the donor and acceptor and thus leading to both direct and indirect (FRET-sensitized) emissions of the latter. The sensitized component is virtually depolarized and thus the mean $\bar{r}$ for the interrogated molecular population provides a measure of FRET. An acceptor with a large Stokes shift is required. There exists an obvious relationship to method Ie4.

The emission anisotropy is also the basis of FRET determinations

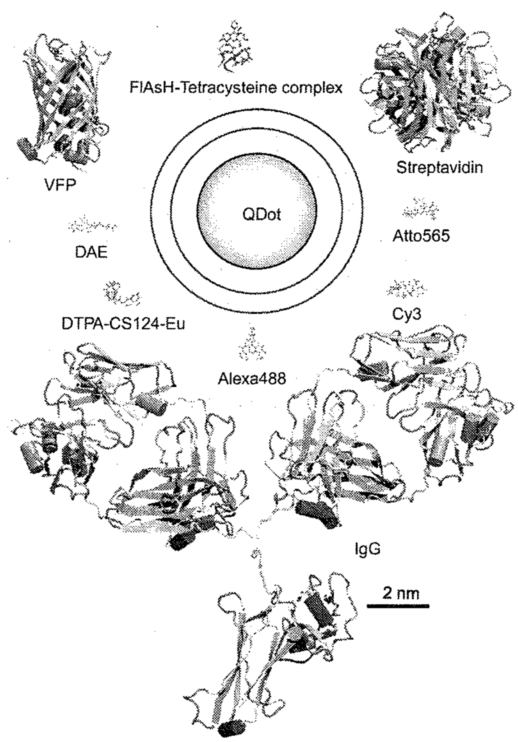

Figure 4 Comparative sizes of common fluorophores and protein carriers used in FRET imaging. Small molecules are represented with Chem3D Ultra (CambridgeSoft). Molecular structures of the small dyes were obtained from available crystallographic data or by minimization using molecular modeling (MM2). DAE, DTPA-CS-EU and ATTO correspond to the dithienylethene depicted in **Figure 3**, the complex of DTPA-carbostyryl 124 with europium[70] and a representative of the Atto dye family (Atto-Tec), respectively. The FlAsH compound is shown as a complex with a 32 amino acid peptide containing a CCGPCC target[39]. The scale bar applies to all molecules. Information required for the depiction of the quantum dot (core, shell, and cap of Qdot 585 Streptavidin Conjugate) was kindly provided by Marcel Bruchez of Quantum Dot. We are greatly indebted to Reinhard Klement for the protein and peptide representations.

measuring the distribution of excited-state energy between identical molecules in close proximity, a process termed homotransfer (or energy migration) RET. EmFRET (our notation[31]) constitutes a sensitive measure of bulk concentration (in the 0.1–10 mM range) and/or of molecular association and clustering in solution (three dimensions) or in planar membranes (two dimensions). One can readily distinguish, for example, between dimerizing and monomeric VFPs with this technique[32]. The depolarization is due to the loss of orientational correlation between excitation and emission but leaving the ensemble lifetime and spectra unaltered. We have demonstrated emFRET in bacteria expressing VFPs[20,31] and in signal transduction mediated by growth factors and their cognate receptor tyrosine kinases fused with VFPs[32] (for other applications, see references in **Table 1**; IIb1,2). One great advantage of emFRET is the requirement for the expression *in vivo* of only a single VFP or other expression probe, as opposed to the requirement for two distinct donor and acceptor molecules in heterotransfer RET. In biotechnological applications, the ability to determine concentrations at the microscopic scale using a dimensionless parameter should be of considerable interest.

In summary, both static (IIb1) and dynamic (IIb2) anisotropies can

Box 1 Photophysical primer

One can regard a given fluorophore as a photophysical catalyst that in a real functional sense shares many attributes of a protein catalyst (an enzyme). That is, the steady-state formalism of the familiar Michaelis-Menten kinetics applies directly to the transformation by a fluorophore F of its 'substrate'—a photon (of wavelength λ_1 and energy hc/λ_1; h, Planck's constant; and c, velocity of light)—that 'binds' (is absorbed) into a 'product'—a photon at longer wavelength λ_2 (and of lesser energy hc/λ_2) with an efficiency dictated by alternative nonradiative pathways (**Fig. 2**).

At low 'substrate concentration,' the rate of photon emission is linearly dependent on light intensity, or more precisely, photon flux Ψ (photons s^{-1} cm^{-2}) = 5×10^{15} irradiance (W cm^{-2}) × wavelength (nm). The photonic 'K_M', the value of Ψ yielding half the maximal fluorescence signal, is given by $[\sigma\tau]^{-1}$, where σ is the absorption cross-section (a measure of photon capture probability, a quantity proportional to the decadic molar absorption coefficient ε; $\sigma = 3.8 \times 10^{-21}\varepsilon$), and τ is the first excited singlet state ($S_1 = F^*$) lifetime; $\tau = k_d^{-1} = [k_f + k_{nr}]^{-1}$; k_f and k_{nr} are the radiative and nonradiative deactivation rate constants, respectively, excluding for the moment other competing processes described below. The initial slope (emission versus excitation photon flux), equivalent to the enzymatic k_{cat}/K_M, is given by σQ; the fluorescence quantum yield (Q) is defined as the ratio of emitted to absorbed photons or by the equivalent expression $k_f/k_d = k_f\tau$. The process saturates at high 'substrate concentration' (irradiance; **Fig. 2**) because the fluorophore is maintained in the excited singlet state (assuming the absence of a finite triplet steady-state population), thus yielding a maximal 'turnover' rate equal to k_f. This maximal rate of fluorescence emission, given by the reciprocal of the radiative lifetime, is independent of Q and of the excitation light intensity and stability, implying that the most sensitive, quantitative, rapid and possibly simplest determination of molecular number, local density or concentration may often be achieved by operating at saturation instead of in the low, linear, range universally espoused for quantitative biological microscopy.

The total photon yield/fluorophore/pulse (PY) for a rectangular excitation pulse of length $t = \alpha\tau$, and photon flux $\psi = \beta/(\sigma\tau)$ is given by equation (4), in which PY_{on} and PY_{off} are the integrated photon emissions during the light (irradiation) and dark (post-irradiation decay) phases, respectively. For $\beta >> 1$ (the saturation condition): $PY \rightarrow Q(1+\alpha)$ and the ratio function OnOff $\rightarrow \alpha$. If α is also >>1 (that is, $t >> \tau$) $PY \rightarrow Q\alpha \equiv k_f t$, confirming the result derived above from the steady-state solution in **Figure 2**.

$$PY = \frac{Q\beta\left[\alpha + (1 + \alpha - e^{-\alpha(1+\beta)})\beta\right]}{(1+\beta)^2} = PY_{on} + PY_{off}$$

$$PY_{on} = \frac{Q\beta\left[e^{-\alpha(1+\beta)} - 1 + \alpha(1+\beta)\right]}{(1+\beta)^2};\; PY_{off} = \frac{Q\beta(1 - e^{-\alpha(1+\beta)})}{1+\beta}$$

$$\mathrm{OnOff} = \frac{PY_{on}}{PY_{off}} = \frac{\alpha}{1 - e^{-\alpha(1+\beta)}} - \frac{1}{1+\beta} \qquad (4)$$

Saturation can be achieved to any desired degree by selection of light pulses of a given repetition rate, duty cycle and duration. These parameters are generally selected so as to reduce background, triplet state buildup, photodestruction and generation of potentially cytotoxic photoproducts (see valuable discussions in refs. 23,92). One can minimize the latter two reactions by limiting the photon dose (irradiance × exposure time $\propto \alpha\beta$).

According to equation (4), a single fluorescein-like molecule ($\varepsilon = 10^5$ M^{-1} cm^{-1}, $\tau = 4$ ns, $Q = 0.4$) exposed to an 8-ns pulse of 0.2 nJ at 488 nm focused to an area of 1 μm^2 ($\alpha = 2$, $\beta = 9.3$) will on average emit 0.69 photons in the light phase and 0.36 photons in the dark phase; the OnOff ratio, 1.9, is very close to α, in accordance with the limiting cases given for equation (4) (see also **Fig. 1b**). The ratio of PY to a given irradiation 'dose' ($\alpha\beta = 18.5$ photons in the above example) constitutes a measure of 'photon conversion efficiency' and thus of signal-to-background contrast. In the event of significant contributions from scattering and short-lived luminescent components, one may wish to gate detection during the pulsed excitation cycle, thereby restricting the signal to PY_{off}.

Photobleaching limits the number of cycles (photon 'turnovers') to $\sim\tau_{pb}/\tau$, in which τ_{pb} is the reciprocal photobleaching rate (**Fig. 5**). A typical value is $\sim 10^5$ cycles (fluorescein), implying that $\sim 10^2$ repetitions would be possible for single determinations based on 10^3 excitation pulses. On the other hand, photobleaching can also be exploited to obtain information, as in determinations of FRET (pbFRET, Id1 and Id2, **Table 1**) and of translational diffusion (FRAP, FLIP[86] and FLAP[93]).

To explore quantitatively the region of saturation (that is, depletion of the ground state), we are obliged to expand the formalism to account for transitions to and from the triplet state, RET between donor and acceptor fluorophores and photobleaching (**Fig. 5a**). The corresponding rate equations for a complete kinetic scheme are first-order except for the virtual second-order RET reaction involving donor* (D*) and acceptor (A) in the forward and acceptor* (A*) and donor (D) in the reverse direction. We circumvent this difficulty by representing the system in terms of transitions between donor-acceptor pairs in the different electronic states (**Fig. 5b**), thereby obtaining analytical expressions that permit the exploration of arbitrary degrees of saturation of both donor and acceptor (see also ref. 29).

report changes in conformation, association and FRET. These techniques are being implemented in numerous microscope systems, most recently in a confocal laser scanning microscope adapted with dual channel polarization detection[32].

Probes and strategies

Solely from the standpoint of stability and brilliance of a fluorophore, one can define a 'figure of merit,' such as the product $\sigma k_f Q_f Q_{pb}^{-1} Q_{isc}^{-1} = \sigma Q_f^2 [\tau Q_{bl} Q_{isc}]^{-1}$. The commercial sources stress σ and Q_f, as exemplified by the cyanines (Amersham Biosciences), Alexa (Molecular Probes) and the long-wavelength Atto (Atto-Tec) series of dyes. However, other considerations apply depending on the FRET method adopted for use (**Table 1**). For example, in donor pbFRET (Id1,Id2) excessive photostability is undesirable, whereas for the methods based on ground state depletion by intersystem crossing (Ic4,Id3), Q_{isc} must be finite. It may also be necessary to tailor the donor lifetime in relation to the dynamics of the particular process under investigation, and although in most cases a large Stokes shift is desirable so as to minimize crossover of the donor fluorescence into the acceptor emission band, a small Stokes shift is required for homotransfer FRET (IIb). Another consideration is the

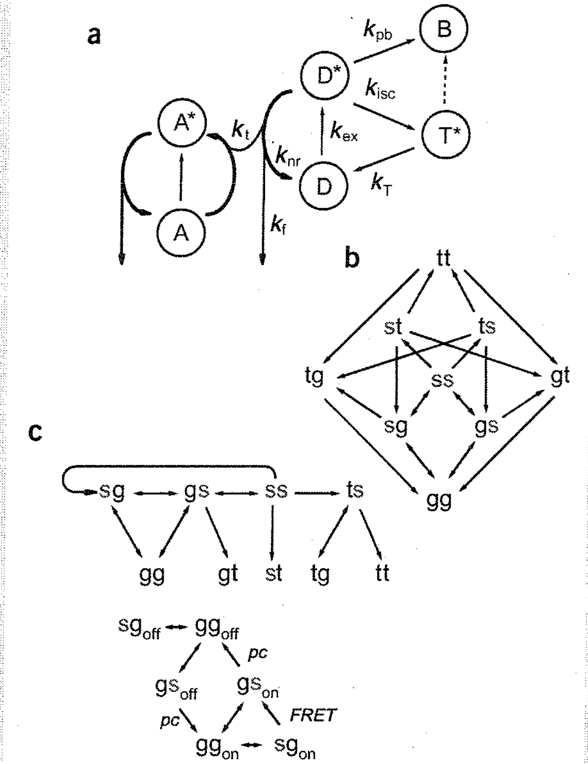

Figure 5 Photophysical cycles including triplet state, FRET, and photobleaching. (**a**) Coupling of donor and acceptor. For simplicity, only the triplet and bleached states of the donor, D, are indicated; the rate constants for the acceptor, A, are also omitted. Definition of rate constants: $k_{ex} = \sigma\psi$; k_{isc}, intersystem crossing (D*→T* transfer); $k_T = \tau_T^{-1}$, triplet decay; k_t, FRET (D*→A* transfer); k_{pb}, photobleaching (can also involve T*). For the usual nanosecond fluorophores lacking heavy atom substituents, k_{isc}, k_{pb}, k_T are << k_f, k_{nr}. (**b**) Photophysical state diagram based on twofold D-A combinations. Each pair consists of a D (left) and A (right) in any of four states: ground (g), excited singlet (blue, red and green s), excited triplet (t) and bleached (not shown). All transitions except FRET are depicted. (**c**) Cycle involving acceptor states excited exclusively via FRET (top), shown as the double-headed arrow (forward and reverse transfer) between sg and gs, and (bottom) of FRET-linked photochromic cycle depicted in **Figure 3**. Analytical, albeit complex, solutions for the corresponding time-dependent and stationary states for the schemes of **b** and **c** have been obtained with Mathematica, including arbitrary degrees of saturation of the D and/or A and explicit consideration of the FRET-excited acceptor species, thereby permitting the calculation of the time course of acceptor anisotropy.

means by which the probe is linked to the target molecule. One might wish to constrain the κ^2 conundrum by introducing flexibility, yet in anisotropy-based FRET determinations (IIb) rigidity is preferable, such as with the bisarsenylated fluorescein (FlAsH; see below) and bifunctional[33] probes. Similar considerations apply to the acceptor, with which the spectral overlap and absorptivity of the acceptor dictate the sensitivity to distance modifications in a given range. However, in cases where the range of lower donor-acceptor separations is of interest, a smaller Γ_0 (that is, J) may be required so as to define a 'working region' optimized around the value $\theta = 1$; see **Figure 1a**.

Current expression probes for determining molecular concentration, distribution and 'age' *in vivo* are primarily based on protein fusions with VFPs of jellyfish or coral origin (reviewed in refs. 4,5,7); other molecular FRET-active VFP derivatives are also available[34,35]. Recent developments in the VFP field, all of which are relevant for FRET, include mutants with increased spectral range, photoconversion capabilities, improved photostability and brightness, faster maturation rate and suppressed tendency to oligomerize. The advent of a photoactivatable VFP[5] is of particular significance. Localized application of blue light to cells—two-photon activation may also be possible—permits the activation of a fluorescence signal at an arbitrary location and time, an invaluable feature for studies of protein translocation and association.

Many new reporters based on donor-acceptor FRET pairs linked by a moiety that undergoes a conformational change upon binding or modification events have been devised[4,5,7,34]. The resulting perturbation of the FRET signal serves as a monitor of the underlying time-dependent process such as protein (de)phosphorylation or ion binding in the specific cellular compartment. A recent FRET-like addition to the VFP toolbox is bimolecular fluorescence complementation (BiFC), conceived as a means for assessing multiple protein-protein interactions *in vivo* with very low background[36]. Nonfluorescent fragments of spectrally distinct VFPs are fused to different proteins of interest. If the latter associate in the cell, the coupled VFP fragments associate and exhibit fluorescence after a maturation period. This technique joins related complementation strategies for studying protein-protein interactions, such as the protein fragment complementation assay (PCA), and the generation of fluorescence or bioluminescence by intein-mediated protein splicing of fragmented VFP or luciferase, respectively[37]. All of these approaches have potential for FRET-based enhancements or implementations, such as with bioluminescence resonance energy transfer in the case of luciferase (**Table 1**; Ia3). In all the VFP-based techniques, two fundamental problems must be faced, namely the possible functional consequences of overexpression and the need to distinguish between VFP-fused proteins delivered to their natural cellular compartment from nascent, reclaimed and degraded molecules elsewhere in the cell. Total internal reflection microscopy[10,38] and other superresolution techniques (S. Hell, this issue) should be of great utility in this respect.

New strategies and dyes with improved properties will expand the capabilities for *in vivo* FRET applications. The combination of exogenous probes and the expression of small peptide targets offer the advantage of greatly reduced size compared to VFPs (**Fig. 4**) and the versatility offered by the ligand in terms of lifetime, large Stokes shift or other property. One such system is based on specific hexapeptide sequences containing four cysteines and introduced into a target protein of interest. Application of an exogenous, membrane permeable, nonfluorescent probe, such as FlAsH or resorufin (ReAsH) derivatives, leads to binding to the tag and the generation of a specific fluorescent signal[39]. We have devoted great effort to developing functional derivatives of these very promising reagents but consider that additional chemical modifications are required to reduce the background in cellular applications (see also ref. 40). Other potential routes might exploit protein fusions with an anti-fluorophore single-chain antibody fragment[41], novel protein scaffolds ('affibodies'[42]), and a newly reported strategy for introducing unnatural amino acid side chains into proteins[43]. The latter may offer targets for a range of chemical and spectroscopic probes, including those suitable for FRET.

Bioconjugated semiconductor quantum dots offer an alternative to organic molecules as fluorescence probes. Quantum dots are finding widespread application as labeling reagents for cells and macromolecules because of their unique properties and commercial availability[44,45]. Appropriately designed quantum dots are very photostable and

nontoxic, can be excited with one or more[46] photons over a wide spectral range, yet emit in a narrow and programmable spectral range. Quantum dots are typically capped with a polymer bearing specific binding moieties, such as streptavidin, protein G, biotin or conjugatable chemical groups (available through such companies as Quantum Dot or Evident Technologies). We have demonstrated the utility of quantum dots as FRET donors in aqueous systems, a further property of these extraordinary materials that will undoubtedly lead to many applications. An important issue relates to size—whether 'the tail wags the dog'—such that a quantum dot–linked probe would interfere or even abrogate the process under study. A graphical representation designed to convey the relative sizes of various common fluorophores and protein probes compared with a quantum dot is provided in **Figure 4**. One is struck by the extent of the IgG molecule, particularly considering the multistep signal amplification schemes in common use.

Several other probes and small particles are of relevance to FRET applications: (i) transfer probes consisting of diffusible, tyramide-linked fluorophores or haptens rendered reactive by peroxidase fused to a target protein or antibody (*e.g.*, the tyramide signal amplification system offered by Molecular Probes); (ii) photoreactive probes that phototransfer from a given protein to an (unknown) partner, for example, in a photocrosslinking reaction[47] mediated by the PES (photochemical enhancement of sensitivity)-FRET mechanism (**Table 1**, Ie4); (iii) microspheres, nanocrystals and phosphors that can be evaluated on and in cells by virtue of attached ligands, morphology, spectroscopy and/or localization and functional effects; (iv) the photochromic probes described above (**Table 1**, Ie2; **Fig. 3**); (v) cascade FRET[23,48] and photoinducible intramolecular charge transfer[49] probes; and (vi) many versions of 'dark' acceptors with very high σ and consequently large Γ_0 values. An important issue with these and other nonexpression probes is the method of introduction into the molecule and/or the cell.

Perspectives

Single-molecule spectroscopy based on fluorescence has developed since the pioneering work Thomas Hirshfeld in the 1970s and in many instances is implemented with imaging technology. FRET is an essential tool[10,50,51] in this field, and should augment the high-resolution techniques recently exemplified in very elegant studies of myosin V dynamics[33,52]. Attempts to confine single-molecule measurements to nanocavities have succeeded in extending the operational range of fluorescence correlation spectroscopy (FCS) to the heretofore inaccessible micromolar range[53] (W. Webb, this issue). Such cellular structures may be suitable for new FRET implementations in FCS[54] and image correlation spectroscopy[55], as well as two-dimensional FCS spectroscopy based on modulated excitation[56], perhaps exploiting the dramatic enhancements of excitation energy transfer achieved in Fabry–Perot microresonators[57]. Scanning near-field optical microscopy (SNOM) provides many interesting imaging possibilities (A. Lewis, this issue), including a donor-coated 'self-sharpening' scanning tip limiting the extent of the corresponding acceptor array to tens of molecules[58]. The same laboratory has recently reported the integration of quantum dots as FRET-SNOM sources with the prospect of single molecule resolution[59], and a coherent mode of operation extending the transfer distance to 20 nm with implications for quantum computing[60]. In the case of cellular imaging based on FRET, one can predict great utility for highly integrated nanochambers[61] and cellular microarrays[62].

We anticipate that many of the newer approaches for FRET microscopy outlined in **Table 1** will come to fruition, hopefully integrated into the full array of emerging multidimensional microscopy techniques, particularly those adapted for optical sectioning. A concrete application representing a core research activity of our groups[32] is the elucidation of ligand-mediated modulation of receptor-receptor distributions and dynamics[63,64,65] on cell surfaces. The ongoing challenge is to expand further the algorithmic repertoire for dissecting such complex molecular systems into their component contributions. It is axiomatic that the full panoply of temporal, spatial and spectral resolution will be required.

ACKNOWLEDGMENTS

E.A.J.-E. is indebted to the Agencia Nacional de Promoción de la Ciencia y Tecnología (ANPCyT), Fundación Antorchas, Consejo Nacional de Investigaciones Científicas y Técnicas (CONICET), Secretaría de Ciencia, Tecnología e Innovación Productiva (SECyT) and the Universidad de Buenos Aires (UBA) for financial support. T.M.J. was supported by the Max Planck Society, European Union FP5 Projects QLG1-2000-01260 and QLG2-CT-2001-02278, and the Center of the Molecular Physiology of the Brain funded by the German Research Council (DFG). The authors were the recipients of a joint grant from the Volkswagen Foundation for their work on photochromic compounds and acknowledge the contribution of graduate student Luciana Giordano to the research depicted in Figure 4, as well as the efforts of many colleagues over the years in the general area represented by this review. They are also indebted professionally and personally for the inspiration offered by the late Gregorio Weber, the acknowledged father of fluorescence in biology. We thank Rainer Heintzmann, Pedro Aramendía, Carla Spagnuolo and Vinod Subramaniam for critical reading of the manuscript.

COMPETING INTEREST STATEMENT

The authors declare that they have no competing financial interests.

Published online at http://www.nature.com/naturebiotechnology/

1. Wieb Van Der Meer, B., Coker, G. III & Simon Chen, S.-Y. *Resonance Energy Transfer: Theory and Data* (VCH, New York, 1994).
2. Hink, M.A., Bisselin, T. & Visser, A.J. Imaging protein–protein interactions in living cells. *Plant Mol. Biol.* **50**, 871–883 (2002).
3. Hoppe, A., Christensen, K. & Swanson, J.A. Fluorescence resonance energy transfer-based stoichiometry in living cells. *Biophys. J.* **83**, 3652–3664 (2002).
4. Zhang, J., Campbell, R.E., Ting, A.Y. & Tsien, R.Y. Creating new fluorescent probes for cell biology. *Nat. Rev. Mol. Cell Biol.* **3**, 906–918 (2002).
5. Lippincott-Schwartz, J. & Patterson, G.H. Development and use of fluorescent protein markers in living cells. *Science* **300**, 87–91 (2003).
6. Meyer, T. & Teruel, M.N. Fluorescence imaging of signaling networks. *Trends Cell Biol.* **13**, 101–106 (2003).
7. Miyawaki, A. Visualization of the spatial and temporal dynamics of intracellular signaling. *Dev. Cell* **4**, 295–305 (2003).
8. Sekar, R.B. & Periasamy, A. Fluorescence resonance energy transfer (FRET) microscopy imaging of live cell protein localizations. *J. Cell Biol.* **160**, 629–633 (2003).
9. Marriott, G. & Parker, I. (eds.). *Biophotonics, Part A. Methods in Enzymology*, vol. 360 (Academic Press, San Diego, CA, 2003).
10. Marriott, G. & Parker, I. (eds.). *Biophotonics, Part B. Methods in Enzymology*, vol. 361 (Academic Press, San Diego, CA, 2003).
11. Berney, C. & Danuser, G. FRET or no FRET: a quantitative comparison. *Biophys. J.* **84**, 3992–4010 (2003).
12. Andrews, D.L. & Demidov, A.A. (eds.). *Resonance Energy Transfer* (John Wiley & Sons, Chicester, UK, 1999).
13. Valeur, B. *Molecular Fluorescence: Principles and Applications* (Wiley-VCH, Weinheim, 2002).
14. Clegg, R.M. Fluorescence resonance energy transfer and nucleic acids. *Methods Enzymol.* **211**, 353–388 (1992).
15. Clegg, R.M. Fluorescence resonance energy transfer (FRET) in *Fluorescence Imaging Spectroscopy and Microscopy* (eds. Wang, X.F. & Herman, B.) 179–252 (John Wiley & Sons, New York, 1996).
16. Edelhoch, H., Brand, L. & Wilchek, M. Fluorescence studies with tryptophyl peptides. *Isr. J. Chem.* **1**, 216–217 (1963).
17. Clegg, R.M., Holub, O. & Gohlke, C. Fluorescence lifetime-resolved imaging: measuring lifetimes in an image. *Methods Enzymol.* **360**, 509–542 (2003).
18. Förster, T. Delocalized excitation and excitation transer in *Modern Quantum Chemistry Part III: Action of Light and Organic Crystals* (ed. Sinanoglu, O.) 93–137 (Academic Press, New York, 1965).
19. Volkmer, A., Subramaniam, V., Birch, D.J. & Jovin, T.M. One- and two-photon excited fluorescence lifetimes and anisotropy decays of green fluorescent proteins. *Biophys. J.* **78**, 1589–1598 (2000).
20. Subramaniam, V., Hanley, Q.S., Clayton, A.H.A. & Jovin, T.M. Photophysics of green and red fluorescent proteins: implications for quantitative microscopy. *Methods Enzymol.* **360**, 178–201 (2003).
21. Patterson, G.H., Piston, D.W. & Barisas, B.G. Förster distances between green fluorescent protein pairs. *Anal. Biochem.* **284**, 438–440 (2000).
22. Kuhn, H. in *Physical Methods of Chemistry*, vol. 1 (eds. Weissberger, A. & Rossiter, B.) 579–650 (John Wiley & Sons, New York, 1972).
23. Schönle, A., Hänninen, P.E. & Hell, S.W. Nonlinear fluorescence through intermolecular

energy transfer and resolution increase in fluorescence microscopy. *Ann. Phys. (Leipzig)* **8**, 115–133 (1999).
24. Heintzmann, R., Jovin, T.M. & Cremer, C. Saturated patterned excitation microscopy (SPEM)—a novel concept for optical resolution improvement. *J. Opt. Soc. Am. A* **19**, 1599–1609 (2002).
25. Jovin, T.M. & Arndt-Jovin, D.J. FRET microscopy: digital imaging of fluorescence resonance energy transfer. in *Cell Structure and Function by Microspectrofluometry* (eds. Kohen, E., Hirschberg, J.G. & Ploem, J.S.) 99–117 (Academic Press, London, 1989).
26. Bastiaens, P.I.H. & Jovin, T.M. Fluorescence resonance energy transfer microscopy in *Cell Biology: A Laboratory Handbook*, vol. 3, edn. 2 (ed. Celis, J.E.) 136–146 (Academic Press, New York, 1998).
27. Giordano, L., Jovin, T.M., Irie, M. & Jares-Erijman, E.A. Diheteroarylethenes as thermally stable photoswitchable acceptors in photochromic fluorescence resonance energy transfer (pcFRET). *J. Am. Chem. Soc.* **124**, 7481–7489 (2002).
28. Song, L., Jares-Erijman, E.A. & Jovin, T.M. A photochromic acceptor as a reversible light-driven switch in fluorescence resonance energy transfer (FRET). *J. Photochem. Photobiol. A* **150**, 177–185 (2002).
29. Hänninen, P.E., Lehtelä, L. & Hell, S.W. Two- and multiphoton excitation of conjugate-dyes using a continuous wave laser. *Optics Comm.* **130**, 29–33 (1996).
30. Mekler, V.M. A photochemical technique to enhance sensitivity of detection of fluorescence resonance energy transfer. *Photochem. Photobiol.* **39**, 615–620 (1994).
31. Clayton, A.H.A., Hanley, Q.S., Arndt-Jovin, D.J., Subramaniam, V. & Jovin, T.M. Dynamic fluorescence anisotropy imaging microscopy in the frequency domain (rFLIM). *Biophys. J.* **83**, 1631–1649 (2002).
32. Lidke, D.S. *et al.* Imaging molecular interactions in cells by dynamic and static fluorescence anisotropy (rFLIM and emFRET). *Biochem. Soc. Trans.*, **31**, 1020–1027 (2003).
33. Forkey, J.N., Quinlan, M.E., Shaw, M.A., Corrie, J.E.T. & Goldman, Y.E. Three-dimensional structural dynamics of myosin V by single-molecule fluorescence polarization. *Nature* **422**, 399–404 (2003).
34. Sato, M., Ozawa, T., Inukai, K., Asano, T. & Umezawa, Y. Fluorescent indicators for imaging protein phosphorylation in single living cells. *Nat. Biotechnol.* **20**, 287–294 (2002).
35. Zacharias, D.A., Violin, J.D., Newton, A.C. & Tsien, R.Y. Partitioning of lipid-modified monomeric GFPs into membrane microdomains of live cells. *Science* **296**, 913–916 (2002).
36. Hu, C.D. & Kerppola, T.K. Simultaneous visualization of multiple protein interactions in living cells using multicolor fluorescence complementation analysis. *Nat. Biotechnol.* **21**, 539–545 (2003).
37. Ozawa, T. & Umezawa, Y. Peptide assemblies in living cells. Methods for detecting protein–protein interactions. *Supramol. Chem.* **14**, 271–280 (2002).
38. Riven, I., Kalmanzon, E., Segev, L. & Reuveny, E. Conformational rearrangements associated with the gating of the G protein-coupled potassium channel revealed. *Neuron* **38**, 225–235 (2003).
39. Gaietta, G. *et al.* Multicolor and electron microscopic imaging of connexin trafficking. *Science* **296**, 503–507 (2002).
40. Falk, M.M. Genetic tags for labelling live cells: gap junctions and beyond. *Trends Cell Biol.* **12**, 399–404 (2002).
41. Farinas, J. & Verkman, A.S. Receptor-mediated targeting of fluorescent probes in living cells. *J. Biol. Chem.* **274**, 7603–7606 (1999).
42. Karlström, A. & Nygren, P.-A. Dual labeling of a binding protein allows for specific fluorescence detection of native protein. *Anal. Biochem.* **295**, 22–30 (2001).
43. Chin, J.W. *et al.* An expanded eukaryotic genetic code. *Science* **301**, 964–967 (2003).
44. Wu, X.Y. *et al.* Immunofluorescent labeling of cancer marker Her2 and other cellular targets with semiconductor quantum dots. *Nat. Biotechnol.* **21**, 41–46 (2003).
45. Jaiswal, J.K., Mattoussi, H., Mauro, J.M. & Simon, S.M. Long-term multiple color imaging of live cells using quantum dot bioconjugates. *Nat. Biotechnol.* **21**, 47–51 (2003).
46. Larson, D.R. *et al.* Water-soluble quantum dots for multiphoton fluorescence imaging *in vivo*. *Science* **300**, 1434–1436 (2003).
47. Fancy, D.A. *et al.* Scope, limitations and mechanistic aspects of the photo-induced cross-linking of proteins by water-soluble metal complexes. *Chem. Biol.* **7**, 697–708 (2000).
48. Haustein, E., Jahnz, M. & Schwille, P. Triple FRET: a tool for studying long-range molecular interactions. *Chemphyschem* **4**, 745–748 (2003).
49. Sauer, M. Single-molecule-sensitive fluorescent sensors based on photoinduced intramolecular charge transfer. *Angew. Chem. Int. Ed. Engl.* **42**, 1790–1793 (2003).
50. Michalet, X. & Weiss, S. Single-molecule spectroscopy and microscopy. *C.R. Phys.* **3**, 619–644 (2002).
51. Ishijima, A. & Yanagida, T. Single molecule nanobioscience. *Trends Biochem. Sci.* **26**, 438–444 (2001).
52. Yildiz, A. *et al.* Myosin V walks hand-over-hand: single fluorophore imaging with 1.5-nm localization. *Science* **300**, 2061–2065 (2003).
53. Levene, M.J. *et al.* Zero-mode waveguides for single-molecule analysis at high concentrations. *Science* **299**, 682–686 (2003).
54. Widengren, J., Schweinberger, E., Berger, S. & Seidel, C.A.M. Two new concepts to measure fluorescence resonance energy transfer via fluorescence correlation spectroscopy: theory and experimental realizations. *J. Phys. Chem. A* **105**, 6851–6866 (2001).
55. Rocheleau, J.V., Wiseman, P.W. & Petersen, N.O. Isolation of bright aggregate fluctuations in a multipopulation image correlation spectroscopy system using intensity subtraction. *Biophys. J.* **84**, 4011–4022 (2003).
56. He, Y., Wang, G., Cox, J. & Geng, L. Two-dimensional fluorescence correlation spectroscopy with modulated excitation. *Anal. Chem.* **73**, 2302–2309 (2001).
57. Hopmeier, M., Guss, W., Deussen, M., Gobel, E.O. & Mahrt, R.F. Control of the energy transfer with the optical microcavity. *Int. J. Mod. Phys. B* **15**, 3704–3708 (2001).
58. Shubeita, G.T., Sekatskii, S.K., Dietler, G. & Letokhov, V.S. Local fluorescent probes for the fluorescence resonance energy transfer scanning near-field optical microscopy. *Appl. Phys. Lett.* **80**, 2625–2627 (2002).
59. Shubeita, G.T. *et al.* Scanning near-field optical microscopy using semiconductor nanocrystals as a local fluorescence and fluorescence resonance energy transfer source. *J. Microsc.* **210**, 274–278 (2003).
60. Sekatskii, S.K., Chergui, M. & Dietler, G. Coherent fluorescence resonance energy transfer: construction of nonlocal multiparticle entangled states and quantum computing. *Europhys. Lett.* **63**, 21–27 (2003).
61. Guijt-van Duijn, R.A. *et al.* Miniaturized analytical assays in biotechnology. *Biotechnol. Adv.* **21**, 431–444 (2003).
62. Ziauddin, J. & Sabatini, D.M. Microarrays of cells expressing defined cDNAs. *Nature* **411**, 107–110 (2001).
63. Tramier, M. *et al.* Homo-FRET versus hetero-FRET to probe homodimers in living cells. *Methods Enzymol.* **360**, 580–597 (2003).
64. Krishnan, R.V., Varma, R. & Mayor, S. Fluorescence methods to probe nanometer-scale organization of molecules in living cell membranes. *J. Fluoresc.* **11**, 211–226 (2001).
65. Wallrabe, H., Elangovan, M.A.B., Periasamy, A. & Barroso, M. Confocal FRET microscopy to measure clustering of ligand–receptor complexes in endocytic membranes. *Biophys. J.* **85**, 559–571 (2003).
66. Garini, Y., Katzir, N., Cabib, D. & Buckwald, R.A. Spectral bio-imaging in *Fluorescence Imaging Spectroscopy and Microscopy* (eds. Wang, X.F. & Herman, B.) 87–124 (John Wiley & Sons, New York, 1996).
67. Jares-Erijman, E. & Jovin, T.M. Determination of DNA helical handedness by fluorescence resonance energy transfer. *J. Mol. Biol.* **257**, 597–617 (1996).
68. Hiraoka, Y., Shimi, T. & Haraguchi, T. Multispectral imaging fluorescence microscopy for living cells. *Cell Struct. Funct.* **27**, 367–374 (2002).
69. Elangovan, M. *et al.* Characterization of one- and two-photon excitation fluorescence resonance energy transfer microscopy. *Methods* **29**, 58–73 (2003).
70. Selvin, P.R. Principles and biophysical applications of lanthanide-based probes. *Annu. Rev. Biophys. Biomol. Struct.* **31**, 275–302 (2002).
71. Xu, Y., Piston, D.W. & Johnson, C.H. A bioluminescence resonance energy transfer (BRET) system: application to interacting circadian clock proteins. *Proc. Natl. Acad. Sci. USA* **96**, 151–156 (1999).
72. Gadella, T.W.J. Jr., van der Krogt, G.N.M. & Bisseling, T. GFP-based FRET microscopy in living plant cells. *Trends Plant Sci.* **4**, 287–291 (1999).
73. Schönle, A., Glatz, M. & Hell, S.W. Four-dimensional multiphoton microscopy with time-correlated single-photon counting. *Appl. Opt.* **39**, 6306–6311 (2000).
74. Yu, W., Mantulin, W.W. & Gratton, E. Fluorescence lifetime imaging: new microscopy techniques in *Emerging Tools for Single Cell Analysis* (eds. Durack, G. & Robinson, J.P.) 139–173 (Wiley-Liss, New York, 2000).
75. Harpur, A.G., Wouters, F.S. & Bastiaens, P.I.H. Imaging FRET between spectrally similar GFP molecules in single cells. *Nat. Biotechnol.* **19**, 167–169 (2001).
76. Carlsson, K. & Philip, J. Theoretical investigation of the signal-to-noise-ratio for different fluorescence lifetime imaging techniques. *SPIE Proc.* **4622**, 70–78 (2002).
77. Elson, D.S. *et al.* Wide-field fluorescence lifetime imaging with optical sectioning and spectral resolution applied to biological samples. *J. Mod. Opt.* **49**, 985–995 (2002).
78. Gerritsen, H.C., Asselbergs, M.A.H., Agronskaia, A.V. & van Sark, W.G.J.H.M. Fluorescence lifetime imaging in scanning microscopes: acquisition speed, photon economy and lifetime resolution. *J. Microsc.* **206**, 218–224 (2002).
79. Hanley, Q.S., Arndt-Jovin, D.J. & Jovin, T.M. Spectrally resolved fluorescence lifetime imaging microscopy. *Appl. Spectrosc.* **56**, 155–166 (2002).
80. Calleja, V. *et al.* Monitoring conformational changes of proteins in cells by fluorescence lifetime imaging microscopy. *Biochem. J.* **372**, 33–40 (2003).
81. Knemeyer, J.-P., Herten, D.-P. & Sauer, M. Detection and identification of single molecules in living cells using spectrally resolved fluorescence lifetime imaging microscopy. *Anal. Chem.* **75**, 2147–2153 (2003).
82. Krishnan, R.V., Saitoh, H., Terada, H., Centonze, V.E. & Herman, B. Development of a multiphoton fluorescence lifetime imaging microscopy (FLIM) system using a streak camera. *Rev. Sci. Instrum.* **74**, 2714–2721 (2003).
83. Siegel, J. *et al.* Wide-field time-resolved fluorescence anisotropy imaging (TR-FAIM): imaging the rotational mobility of a fluorophore. *Rev. Sci. Instrum.* **74** (2003).
84. Jovin, T.M. & Arndt-Jovin, D.J. Luminescence digital imaging microscopy. *Annu. Rev. Biophys. Biophys. Chem.* **18**, 271–308 (1989).
85. Young, R.M., Arnette, J.K., Roess, D.A. & Barisas, B.G. Quantitation of fluorescence energy transfer between cell surface proteins via fluorescence donor photobleaching kinetics. *Biophys. J.* **67**, 881–888 (1994).
86. Lippincott-Schwartz, J., Snapp, E. & Kenworthy, A. Studying protein dynamics in living cells. *Nat. Rev. Mol. Cell Biol.* **2**, 444–456 (2001).
87. Kenworthy, A.K. Imaging protein–protein interactions using fluorescence resonance energy transfer microscopy. *Methods* **24**, 289–296 (2001).
88. Matkó, J., Jenei, A., Matyus, L., Ameloot, M. & Damjanovich, S. Mapping of cell surface protein-patterns by combined fluorescence anisotropy and energy transfer measurements. *J. Photochem. Photobiol. B* **19**, 71–73 (1993).
89. Runnels, L.W. & Scarlata, S.F. Theory and application of fluorescence homotransfer to melittin oligomerization. *Biophys. J.* **69**, 1569–1583 (1995).
90. Yan, Y. & Marriott, G. Fluorescence resonance energy transfer imaging microscopy and fluorescence polarization imaging microscopy. *Methods Enzymol.* **360**, 561–580 (2003).
91. Buehler, C., Dong, C.Y., So, P.T.C., French, T. & Gratton, E. Time-resolved polarization imaging by pump-probe (stimulated emission) fluorescence microscopy. *Biophys. J.* **79**, 536–549 (2000).
92. Mathies, R.A., Peck, K. & Stryer, L. Optimization of high-sensitivity fluorescence detection. *Anal. Chem.* **62**, 1786–1791 (1990).
93. Dunn, G.A., Dobbie, I.M., Monypenny, J., Holt, M.R. & Zicha, D. Fluorescence localization after photobleaching (FLAP): a new method for studying protein dynamics in living cells. *J. Microsc.* **205**, 109–112 (2002).

Ion-induced FRET On-Off in fluorescent calix[4]arene

Min Hee Lee,[1] Duong Tuan Quang,[1] Hyo Sung Jung,[1] Juyoung Yoon,[2] and Jong Seung Kim[1,*]

[1]*Department of Chemistry, Institute of Nanosensor & Biotechnology, Dankook University, Seoul 140-714, Korea.*

[2]*Department of Chemistry and Division of Nano Sciences, Ewha Womans University, Seoul 120-750, Korea.*

Corresponding author: jongskim@dankook.ac.kr (J. S. Kim), Fax: +82-2-797-3277

Abstract

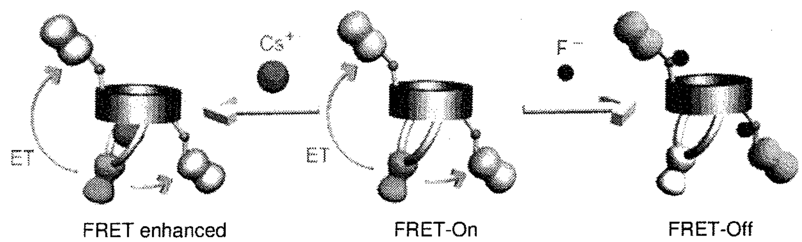

*A novel calix[4]arene bearing one 2,3-naphthocrown-6 and two coumarin amide units at the lower rim in partial-cone conformation (**1**) was synthesized as a colorimetric and FRET-based fluorometric sensor for F^- and Cs^+ ions. Intramolecular FRET from the naphthalene emission to the coumarin absorption affords a high fluorescence selectivity towards F^- and Cs^+ ion.*

Fluorometry is becoming important for ion sensing because of its simplicity, high selectivity and sensitivity.[1] Design of a fluorescence sensor requires a molecule that possesses two functional units: an ionophore responsible for selectively binding ions and a fluorophore responsible for signal transduction. Most fluorometric sensors are designed to adopt photo-physical changes produced upon complexation including photo-induced electron transfer (PET),[2] photo-induced charge transfer (PCT),[3] excimer/exciplex formation and extinction,[4,5] or fluorescence resonance energy transfer (FRET).[6] There are numerous reports concerning ion sensors based on PCT, PET and excimer/exciplex. The FRET is known to be sensitive, selective and adaptable to a wide variety of systems,[7,8] however, the reports on FRET-based ion sensors are still in a modest number.

FRET arises from an interaction between a pair of fluorophores in their excited states. By a long-range dipole-dipole coupling mechanism, the excited state of a fluorescent donor is then non-radiatively transferred to the acceptor and the donor returns to its electronic ground state. Therefore, the FRET is required to have a certain extent of spectral overlap between the donor emission and the acceptor absorption.[9,10]

In previous paper,[11] we reported a calix[4]arene with two coumarin groups at the lower rim acting as a fluoride-selective sensor. The addition of fluoride ion into the compound causes a strong quenching of fluorescence emission with a red shift, which can be explained by photo-induced charge transfer (PCT).

Keeping previous researches above in mind, we thought the attachment of both naphthalene and coumarin groups to the calix[4]arene platform could provide a compound showing that FRET from an excited donor (naphthalene) to a nearby acceptor (coumarin), and the FRET efficiency is variable with an anion added. Besides, the naphthalene group is linked to the calix[4]crown-6 loop, which is capable of binding Cs^+ ion effectively, promoting the

FRET efficiency changes.[12] These two ions have received interest from chemists for their biological and environmental demands. F^- ion is known to be essential to human beings at low concentrations, but potentially toxic at higher levels[13,14] while radio-active Cs^+ ion can damage living organisms.[15]

In this paper, we report the synthesis and the fluorometric properties of a calix[4]arene **1** as well as its sensing ability for both cations and anions with respect to the FRET changes. The colorimetric ion sensing ability is also studied and presented herein.

As shown in Scheme 1, reaction of calix[4]arene with 2,3-naphthoglycolic ditosylate (**2**)[16] under basic medium gave **3** in 30 % yield. Although only 1.0 eq of ditosylate was used, the reaction yield is quite low due to the preferential formation of calix[4]biscrown-6.[16] Synthesis of **1** was performed by the condensation of acylated 7-amino-4-(trifluoromethyl)coumarin (**4**)[11] with *cone*-calix[4]monocrown-6 (**3**) in the presence of Cs_2CO_3 as a base and a catalytic amount of KI. Unexpectedly, we obtained **1** in the *partial-cone* conformation instead of *1,3-alternate* one which may show a stronger binding ability towards alkali metal cation.[12] ^{1}H NMR peaks of **1** at 4.48, 3.75, and 3.22 ppm for 8 hydrogen atoms of ArCH_2Ar and ^{13}C NMR peaks of ArCH_2Ar at 38.02 and 32.07 ppm clearly indicate that it is in the fixed *partial-cone* conformation.[17,18] In order to prove the fact of the CHEF effect and FRET in compound **1**, reference material **5** was also prepared as shown in Scheme 2.

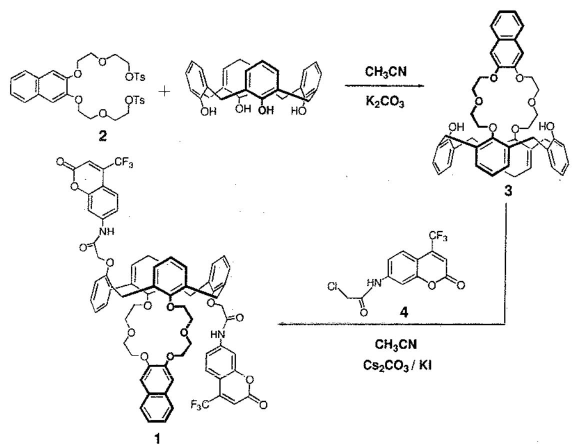

Scheme 1. Synthetic pathways to **1**.

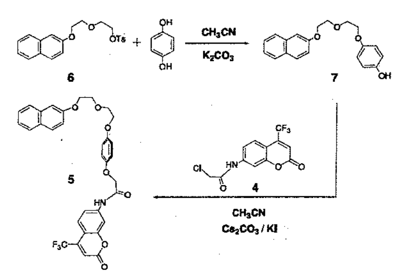

Scheme 2. Synthetic pathways to **5**.

Compound **1** contains two amide groups capable of binding anions[11] and one crown-6 loop as a binding site for metal cations.[12] Free **1** displays two strong absorption bands at 242 and 344 nm arisen from the naphthalene and the coumarin moieties, respectively, which are confirmed by the absorption spectra of the reference materials **3** and **4** (Figure S1). Also, **1** shows weak naphthalene emission bands ranged from 326 to 340 nm along with a broad coumarin

emission band at 422 nm with an excitation at 245 nm (Figure S2). Then the spectral overlap between naphthalene emission and coumarin absorption is optimized to provide the FRET-On. As seen in Figure S1, F^- ion binding promotes a red-shift of coumarin absorption band by 91 nm, which is due to photo-induced charge transfer (PCT).[11] As a result, the spectral overlap between the donor and the acceptor is declined to give the FRET-Off.

Figure 1 shows absorption changes of **1** upon addition of F^-, Cl^-, Br^-, I^-, CH_3COO^-, OH^-, HSO_4^- and $H_2PO_4^-$. Only F^- ion induces a significant red-shift of the coumarin absorption from 344 to 435 nm. Additionally, fluorescence changes of **1** upon the addition of various anions exhibit an especially high selectivity towards fluoride ion (Figure S2). Therefore, we envisioned that these fluorescence and absorption changes associated with the mechanism in Scheme 3 could potentially be applicable to the development of selective chemosensor for fluoride ion in CH_3CN. In the fluoride titration absorption spectra, we can observe two clear isosbestic points at 306 and 372 nm (Figure S3). The red-shift from 344 to 435 nm of the coumarin band is attributed to H-bonding between amide N-H and F^- followed by deprotonation along with a visual color change from colorless to pale yellow. The color change was not observed until amount of fluoride ion added reaches to 20 eq (Figure S4). The color only remained unchanged for short period (less than 5 min) and turned into deep yellow after that. Therefore, all experiments were immediately carried out after preparation of samples.

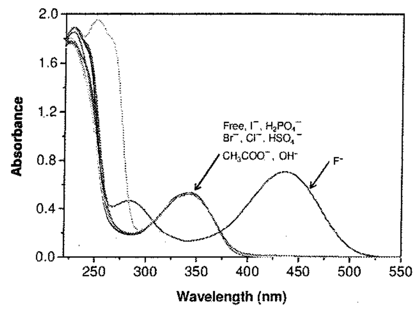

Figure 1. Absorption spectra of **1** (20.0 μM) upon addition of TBA^+ salts of F^-, Cl^-, Br^-, I^-, CH_3COO^-, OH^-, HSO_4^-, and $H_2PO_4^-$ (10.0 mM) in CH_3CN.

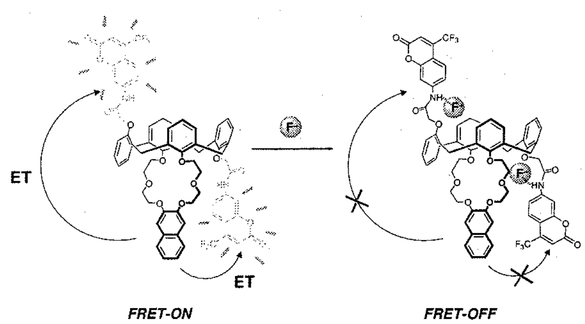

Scheme 3. FRET switch mechanism of **1** with F^-.

Figure 2 indicates fluorescence changes upon fluoride anion titration. Upon addition of F^- in **1**, red-shifted coumarin emissions appear at 536 nm due to PCT mechanism[11] and the naphthalene emission at 342 nm concomitantly revives, which can be referred to FRET-off caused by a minimized spectral overlap between donor emission and acceptor absorption band (Scheme 3 and Figure S1). Addition of 2,000 equiv of F^- gives a quenched coumarin emission, which is presumably due to the photo-induced electron transfer (PET) from F^- to the coumarin unit.

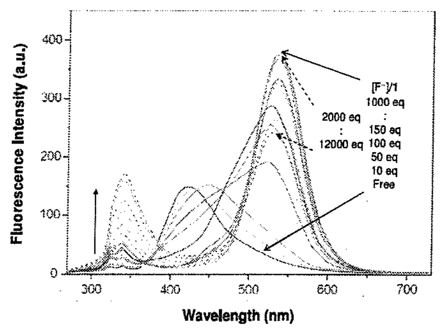

Figure 2. Fluorescence spectra of **1** (6.0 μM) upon addition of various concentrations of TBA^+ F^- in CH_3CN with an excitation at 245 nm.

To gain insight into a role of the calix[4]arene framework in **1** on this FRET effect, the photophysical property of **1**·F^- was compared with that of reference **5**·F^-. As shown in Figure 3, **5** displays a stronger naphthalene emission at 342 nm than does **1**, implying that the FRET efficiency from naphthalene to coumarin in **1** is larger than that in **5**. This is presumably because unlike **5**, **1** with calix[4]arene framework in organic solvent has a greater conformational rigidity with respect to the favorable distance capable of executing the FRET between the naphthalene and the coumarin. Then, addition of F^- to a solution of **1** increases the naphthalene emission because of the FRET declined whereas addition of F^- to **5** rarely changes the naphthalene emission. From the titration experiment, association constants of **1** and **5** for F^- in CH_3CN were calculated to be 5.7×10^4 and 1.9×10^3 M^{-1} (Figures S3, S7 and S8), respectively.[19] For the FRET efficiency, we can also estimate from the following equation.[20]

$$E = 1\text{-}(F'_D/F_D)$$

Where E denotes FRET efficiency; F'_D and F_D are the donor fluorescence intensity with and without acceptor, respectively. E of **1**, **5**, **1**·F^-, and **5**·F^- were calculated to be 0.95, 0.66, 0.79 and 0.62, respectively. So, it is noteworthy that the FRET change of **1** with calixarene platform is more considereable than that of **5** in the presence of F^-, which means **1** responds to F^- ion more sensitively than **5** does.

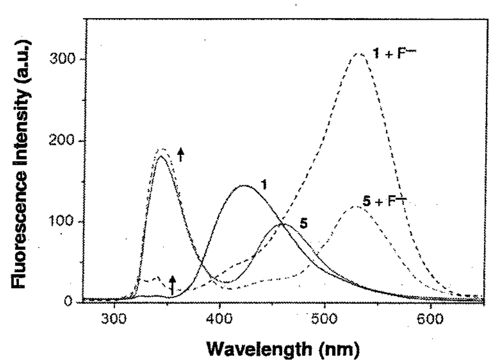

Figure 3. Fluorescence spectra of **1** (6.0 μM) and **5** (6.0 μM) upon addition of TBA^+ F^- in CH_3CN with an excitation at 245 nm. Solid line: ligand only; dashed line: ligand + F^- (0.6 mM)

For the binding interaction between **1** and fluoride ion, NMR tirations of the $CDCl_3$ solution of **1** with fluoride ion were carried out (Figure S9). The intensity of the amide proton signal continuously decreases with addition of fluoride ion and vanishes at 0.58 eq, which can be explained by N-H deprotonation promoted by: (i) the intrinsic acidity

of **1** enhanced by conjugation of nitrogen lone-pair electrons with the aromatic ring and (ii) the high stability of $[HF_2]^-$ hydrogen bonding complex.

In addition to evaluating a response of **1** for anions, those for cations using perchlorate salts were also carried out. There is no significant absorption change of **1** in intensity as well as in wavelength upon addition of cations (Figure S10). The fluorescence intensity changes (I - I_0) of both **1** and **5** upon addition of various cations are listed in Figure 4. The results indicate that **1** exhibits a high selectivity for Cs^+ ion. It is known that the Cs^+ ion is favorably encapsulated in the calixcrown-6-ether ring and the K^+ ion prefers to be encapsulated in the crown-5-ether ring because of the size complementarities along with the π-metal interaction concept.[12] Association constants of **1** for Cs^+ and K^+ ions estimated from spectrophotometric titrations are 5.4×10^2 and 1.6×10^2 M^{-1}, respectively.[19]

Interestingly, we here also observed that the coumarin emission of **1** is markedly enhanced when Cs^+ ion is added to a solution of **1**. This is because the CHEF (chelating enhanced fluorescence) upon complexation with Cs^+ ion leads to the repression of the PET from oxygen atoms to the naphthalene group, making the spectral overlap (FRET) between donor emission (naphthalene) and acceptor absorption (coumarin) more effective. In contrast, reference **5** which has neither crown-6 nor calix[4]arene does not show any fluorescence changes under the same condition, confirming that the calixcrown-6 part plays a key role in Cs^+ ion binding to enhance the FRET efficiency.

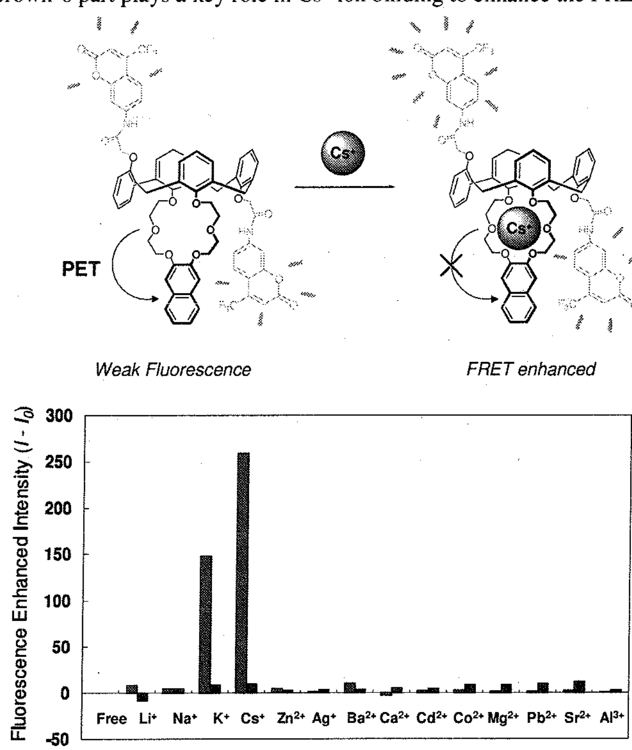

Figure 4. Complexation mechanism of **1** with Cs^+ ion and fluorescence enhanced intensity (λ_{em}=422 nm) of **1** (6.0 μM, red) and **5** (6.0 μM, blue) upon addition of various metal ions (3.0 mM) in CH_3CN with an excitation at 245 nm.

In conclusion, FRET-based colorimetric and fluorometric calix[4]arene was developed. The FRET efficiency generated from naphthalene to coumarin in **1** is larger than that in **5**. The F^- selectivity over other anions was observed from the extent of the FRET change of **1**. Besides, regarding the FRET changes, we observed that **1** also shows Cs^+ ion selectivity over other metal cations. Addition of Cs^+ ion to **1** provides an enhanced FRET in **1** because repression of the

PET induces the spectral overlap between donor emission and acceptor absorption more efficiently.

Experimental section

Synthesis. Compounds **2**,[16] **3**,[16] **4**,[11] and **6**[16] were prepared by following the methods reported earlier.

Preparation of 1. Under nitrogen, a solution of **3** (1 g, 1.38 mmol), **4** (1.26 g, 4.14 mmol), Cs_2CO_3 (0.67 g, 2.07 mmol) and a catalytic amount of KI in CH_3CN (20 mL) was heated at 80^0C. After refluxing for 24 h, the mixture was dissolved in CH_2Cl_2 (100 mL) and treated with dilute HCl. The organic layer was washed with water (300 mL), dried over anhydrous $MgSO_4$ and filtered. Purification by chromatography on silica gel (ethyl acetate/hexane, 1:2) allowed the isolation of **1** as yellowish solid in 20 % (0.34 g) yield. Mp 178-180 ℃. IR (KBr pellet, cm^{-1}): 1650, 1725, 1515. FAB MS *m/z* (M^+) calcd 1262.3, found 1263.0. Anal. Calcd for $C_{70}H_{56}F_6N_2O_{14}$: C, 66.56; H, 4.47; N, 2.22. Found: C, 66.56; H, 4.65; N, 2.12.

Preparation of 5. Under nitrogen, a solution of **7** (0.3 g, 0.92 mmol), **4** (0.43 g, 1.43 mmol), Cs_2CO_3 (0.13 g, 0.92 mmol) in CH_3CN (30 mL) was heated at 80^0C. After refluxing for 24 h, the mixture was dissolved in CH_2Cl_2 (100 mL) and treated with dilute HCl. The organic layer was washed with water (300 mL), dried over anhydrous $MgSO_4$ and filtered. Recrystallization from MeOH produced 0.3 g (60 %) of **5** as a yellow solid. Mp 130-132 ℃. IR (KBr pellet, cm^{-1}): 1720, 1121. FAB MS *m/z* (M^+) calcd 593.5, found 594.0. Anal. Calcd for $C_{32}H_{26}F_3NO_7$: C, 65.75; H, 4.42. Found: C, 65.76; H, 4.40.

Preparation of 7. Under nitrogen, a solution of hydroquinone (0.3 g, 2.7 mmol), **6** (1.05 g, 2.7 mmol), K_2CO_3 (0.19 g, 1.4 mmol) in CH_3CN (30 mL) was heated at 80^0C. After refluxing for 24 h, the mixture was dissolved in CH_2Cl_2 (100 mL) and treated with 5 % aqueous HCl solution. The organic layer was washed with water (300 mL), dried over anhydrous $MgSO_4$ and filtered. Purification by chromatography on silica gel (ethyl acetate/hexane, 1:4) allowed the isolation of **7** as colorless oil in 50 % (0.45 g) yield. IR (KBr pellet, cm^{-1}): 3400, 1615, 1112. FAB MS *m/z* (M^+) calcd 324.3, found 324.0. Anal. Calcd for $C_{20}H_{20}O_4$: C, 74.06; H, 6.21. Found: C, 74.09; H, 6.20.

Acknowledgment: This work was supported by the SRC program (R11-2005-008-02001-0(2006)) and Basic Science Research of KOSEF (R01-2006-000-10001-0).

Supporting Information Available: Additional UV/Vis, fluorescence, and NMR spectra, and calculation data are available free of charge *via* the Internet at http://pubs.acs.org.

References

1. (a) Kim, S. K.; Lee, S. H.; Lee, J. Y.; Lee, J. Y.; Bartsch, R. A.; Kim, J. S. *J. Am. Chem. Soc.* **2004**, *126*, 16499. (b) Kim, S. K.; Bok, J. H.; Bartsch, R. A.; Lee, J. Y; Kim, J. S. *Org. Lett*. **2005**, *7*, 4839. (c) Cho, E. J.; Moon, J. W.; Ko, S. W.; Lee, J. Y.; Kim, S. K.; Yoon, J.; Nam, K. C. *J. Am. Chem. Soc.* **2003**, *125*, 12376.
2. (a) Aoki, L.; Sakaki, T.; Shinkai, S. *J. Chem. Soc., Chem. Commun.* **1992**, 730. (b) Jin, T.; Ichikawa, K.; Koyama, T. *J. Chem. Soc., Chem. Commun.* **1992**, 499. (c) Ji, H.-F.; Brown, G. M.; Dabestani, R. *Chem. Commun.* **1999**, 609. (d) Kim, J. S.; Shon, O. J.; Rim, J. A.; Kim, S. K.; Yoon, J. *J. Org. Chem.* **2002**, *67*, 2348. (e) Kim, J. S.; Noh, K. H.; Lee, S. H.; Kim, S. K.; Kim, S. K.; Yoon, J. *J. Org. Chem.* **2003**, *68*, 597.
3. Leray, I.; Lefevre, J. P.; Delouis, J. F.; Delaire, J.; Valeur, B. *Chem. Eur. J.* **2001**, *7(21)*, 4590.
4. Birks, J. B. *Photophysics of Aromatic Molecules*; Wiley-Interscience: London, 1970.
5. Lee, S. H.; Kim, S. H.; Kim, S. K.; Jung, J. H.; Kim, J. S. *J. Org. Chem.* **2005**, *70*, 9288.

6. Hecht, S.; Vladimirov, N.; Fréchet. J. M. J. *J. Am. Chem. Soc.* **2001**, *123*, 18.
7. Tsien, R. Y.; Miyawaki, A. *Science* **1998**, *280*, 1954.
8. Weiss, S. *Science* **1999**, *283*, 1676.
9. Lakowicz, J. R., Ed. *Principles of Fluorescence Spectroscopy*; Plenum Publishers Corporation: New York, 1999.
10. Stryer, L.; Haugland, R. P. *Proc. Natl. Acad. Sci. USA* **1967**, *58*, 719.
11. Lee, S. H.; Kim, H. J.; Lee, Y. O.; Vicens, J.; Kim, J. S. *Tetrahedron Lett.* **2006**, *47*, 4373.
12. Casnati, A.; Ungaro, R.; Asfari, Z.; Vicens. J. In *Calixarenes 2001*: Asfari, Z.; Böhmer, V., Harrowfield, J., Eds.; Kluwer Academic Publishers: Dordrecht, The Netherlands, 2001; p 365.
13. Camargo, J. A. *Chemosphere* **2003**, *50*, 251.
14. Cerklewski, F. L. *Nutr. Res.* **1997**, *17*, 907.
15. Gaur, S. *J. Chromatogr. A* **1996**, *733*, 57.
16. (a) Asfari, Z.; Bressot, C.; Vicens, J.; Hill, C.; Dozol, J-F.; Rouquette, H.; Eymard, S.; Lamare.; Tournois, B. *Anal. Chem.* **1995**, *67*, 3133. (b) Zouhair, A.; Pierre, T.; Martine, N.; Vicens, J. *Tetrahedron Lett.* **1999**, *40*, 499.
17. Neri, P.; Bottino, A.; Geraci, C.; Piattelli, M. *Tetrahedron: Asymmetry* **1996**, *7*, 17.
18. Louati, A.; Spraula, J.; Gabelica, V.; Kuhn, P.; Matt, D. *Electrochem. Commun.* **2006**, *8*, 761.
19. (a) Association constants were calculated using the conputer program ENZFITTER, available from Elsevier-BIOSOFT, 68 Hills Road, Cambridge CB2 1LA, United Kingdom. (b) Connors, K. A. *Binding Constants*; Wiley: New York, 1987.
20. Lakowicz, J. R. *Principles of Fluorescence Spectroscopy*, 2nd ed.;1999; Chapter 13.

Synthesis of indole-containing diheteroarylethenes. New probes for photochromic FRET (pcFRET)

Luciana Giordano[1], Rudolf J. Vermeij[2], and Elizabeth A. Jares-Erijman[1,*]

[1.] Departamento de Química Orgánica. Facultad de Ciencias Exactas y Naturales. Universidad de Buenos Aires. Ciudad Universitaria Pabellón II Buenos Aires. Argentina. [2] Department of Molecular Biology, Max Planck Institute for Biophysical Chemistry, 37077 Göttingen, Germany Present address: MESA+ Institute for Nanotechnology, Faculty of Science and Technology, University of Twente, PO Box 217, 7500 AE Enschede, The Netherlands.
Email: eli@qo.fcen.uba.ar

Dedicated to Professor Rosa M. de Lederkremer

Abstract
This paper reports a synthesis of novel diheteroarylethenes functionalized for coupling to biomolecules starting from indole derivatives. The strategy is based on the derivatization at the N-atom in the indole substructure. TBDMS protection proved to be superior over BOC protection schemes, leading to higher yields in the overall synthesis. The suitability of the new derivatives as acceptors for pcFRET was calculated for selected donors.

Keywords: Photochromism, FRET, diheteroarylethenes, synthesis, indole derivatives

Introduction

Photochromism is the result of reversible photoisomerization between two isomers that have distinct absorption spectra. The two isomers differ from one another not only in their absorption spectra but also in other physical and chemical properties.[1] Among the different photochromic compounds diheteroarylethenes are excellent candidates for optoelectronic devices due to their fatigue resistance and thermally irreversible conversion.[2]

Diheteroarylethenes undergo isomerization from an open to a closed form (scheme 1) upon irradiation with UV light. Visible light converts the closed form back into the original open form. Symmetric indole- or pyrrole containing diheteroarylethenes give rise to thermally unstable closed form isomers. By replacing one indole with a furane, thiophene or benzothiophene group, the asymmetric diheteroarylethene becomes thermally stable in the closed form. A number of methyl indole derivatives have been introduced by Irie and coworkers[3] and the resulting

photochromic compounds display interesting optical properties which makes them suitable as acceptors for energy transfer for a variety of fluorophore donors.

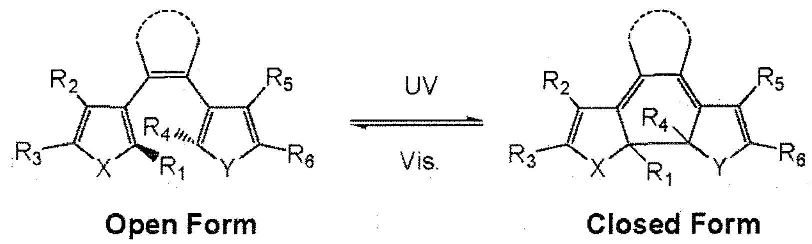

Scheme 1

FRET (Förster Resonance Energy Transfer) is a physical process by which energy is transferred non-radiatively from an excited molecular fluorophore (donor) to another chromophore (acceptor) via long-range dipole-dipole coupling. The FRET acceptor need not be fluorescent, but must fulfill the requirements of having an absorption spectrum overlapping the emission spectrum of the donor with the respective transition moments in a favorable, i.e. non-orthogonal, relative orientation. We have shown previously that diheteroarylethenes can be used as acceptors for photochromic Förster Resonance Energy Transfer (pcFRET),[4, 5] a technique developed to perform the quantitative determination of FRET *in vivo*. The photochromic compound is converted from a colorless open form to a FRET-competent acceptor closed form upon irradiation with ultraviolet (UV) light. The open form lacks absorbance in the visible range. Thus, the overlap with the emission of the donor is negligible. The closed form has an absorption band overlapping the emission band of the donor, which can be switched back to the open, non-overlapping form by exposure to visible light. Multiple "on"/"off" FRET cycles can be generated by alternating exposure to UV and visible light.

Application of photochromic compounds as pcFRET acceptors in biology requires that they contain functional groups that can be used for their conjugation to (bio)molecules. Indole derivatives offer the opportunity for preparing a functionalized substituent on the N atom. Here we report the synthesis of asymmetric diheteroarylethenes bearing a removable protecting group at this position.

The diheteroarylhexafluorocyclopentenes are usually obtained by a reaction involving nucleophilic attack of a heteroaryllithium on octafluorocyclopentene, followed by elimination of fluoride groups.[2, 6] With indole as one of the heteroaryl functionalities, the heteroaryllitium species can be formed by halogen-lithium exchange reaction of the *N*-protected 3-haloindoles. Synthesis of these haloindoles is usually performed by electrophilic substitution. *N*-Protection of the indoles can be carried out before or after the halogenation step. As a result, the requirements of the protecting group are dictated by the lithium-halogen exchange reaction conditions. The synthesis and application of these *N*-protected indoles is well documented:[7, 8] alkyl, silyl, alkoxymethyl, acyl and other protecting groups have been used. Here we investigated their use for reaction with perfluorocyclopentene.

Results and Discussion

The first class of protective group investigated in this synthetic approach was the *t*-butoxycarbonyl group (BOC) (Scheme 2). 3-Iodo-2-methylindole **2** was obtained by iodination of 2-methylindole **1**[9,10] which was followed by protection of the *N*-position of the indole nucleus to give **3**. In order to assess the best reaction conditions, different stoichiometric relationships between *n*-butyllithium and the alkylating reagent CH_3I were tested (reaction not shown in Scheme). The best yields (65-86%) were obtained when 2 equivalents of *n*-butyllithium and 1.5-3 equiv of CH_3I were used at -30 °C. Lithiation of the 3-iodoindole **3**, followed by reaction with excess octafluorocyclopentene led to compound **4** in 42% yield. However, when a similar substitution reaction of the lithiated indole with compound **7** was attempted, the reaction proceeded sluggishly and only 29% of the desired product (**5**) was isolated, recovering 50% of starting material. When excess *n*-butyllithium was used in the halogen-metal exchange reaction, the desired product was isolated in 20% yield. In addition, the side product from reaction of unreacted *n*-butyllithium with **7** gave **6** in 48% (based on **7**).

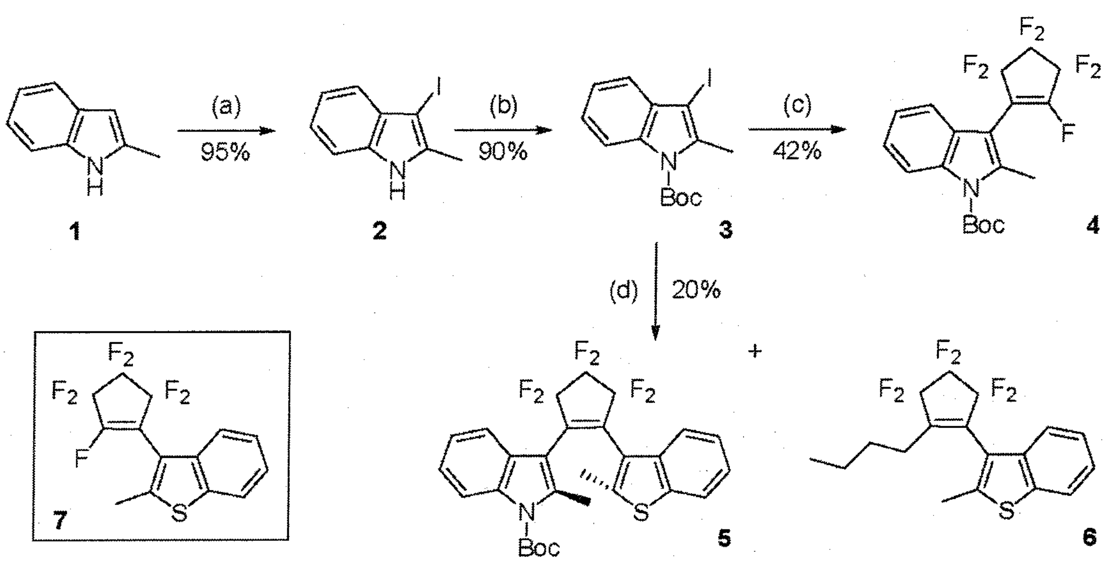

a) KOH / I_2 / DMF b) Boc_2O / TEA / DMAP / CH_2Cl_2 c) i) *n*-BuLi (2.2 eq) / THF / -78 °C ii) C_5F_8 d) i) *n*-BuLi (2.2 eq) / THF / -78 °C ii) **7**

Scheme 2

TBDMS was applied in an alternative protection strategy (Scheme 3). 2-Methylindole derivatives **1** and **8** were deprotonated with NaH and protected with TBDMSCl yielding **9** and **10**. Bromination with NBS at –78 °C gave **11** and **12**.[11]

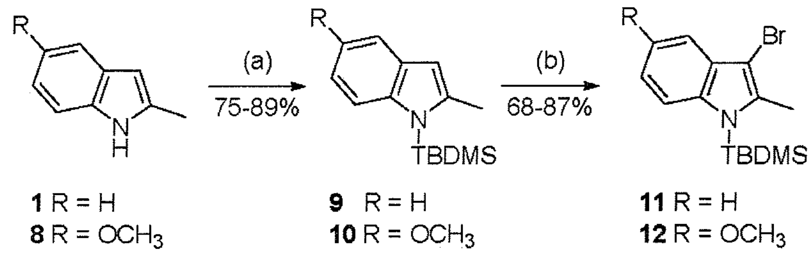

a) i) NaH / THF ii) TBDMSCl b) NBS / THF / -78 °C

Scheme 3

Lithiation of compounds **11** and **12** with *n*-butyllithium at –78 °C, followed by reaction with **7** or **16** (**11** only) rendered the desired diheteroarylethenes **13** – **15** in reasonable yields (Scheme 4). These compounds already contain the photochromic moiety and bear orthogonally protected phenolic (OH; **14 only**) and indolic (NH) functionalities suitable for further derivatizations.

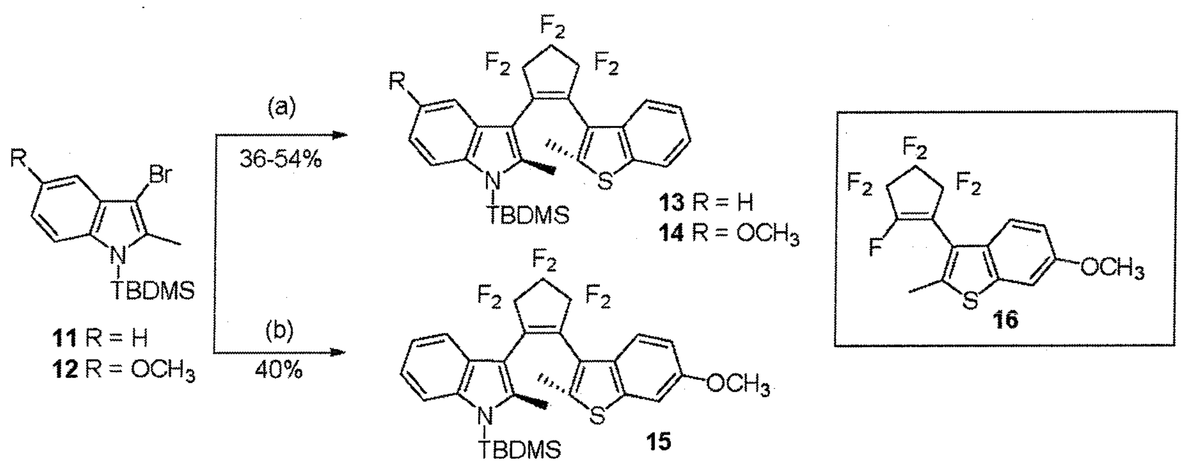

a) i) *n*-BuLi / THF / -78 °C ii) **7** b) i) *n*-BuLi / THF / -78 °C ii) **16**

Scheme 4

Deprotection of the indole-nitrogen proceeded smoothly with TBAF (Scheme 5). Immediate reaction with NaH followed by alkylation with ethyl bromoacetate in DMF rendered **18**, which by hydrolysis gave the final product **19**.[12, 13] Compound **19** contains a carboxylic acid group that can be further activated for conjugation with amine groups.

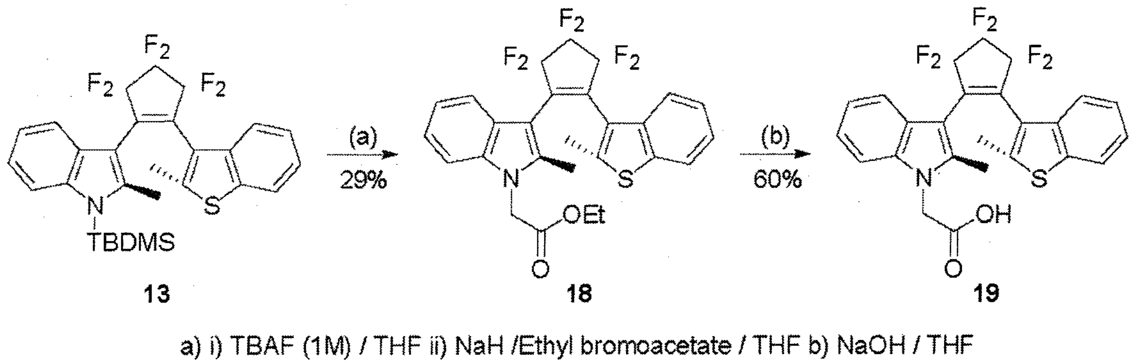

Scheme 5

Absorption properties. The absorption spectra of the open- and the closed forms are shown in Figure 1 **a** and **b**, respectively.

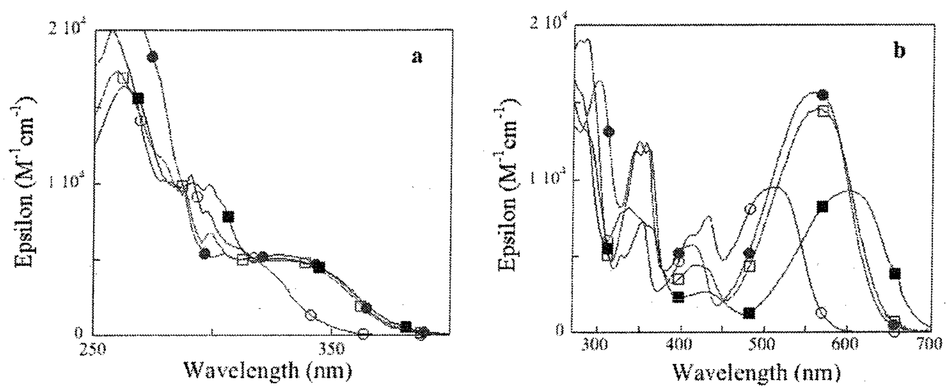

Figure 1. Absorption properties of compounds **5** (blue empty circles), **13** (red empty squares), **14** (black full squares), **15** (green full circles), in the open (**a**), and in the closed (**b**) form, respectively.

The optical properties of compounds **5**, **13-15** are given in Table I summarizing the absorption maxima corresponding to the open and closed forms, emission maxima of the open form, and the fractional conversion (to the closed form) achieved in the photostationary state by irradiation at the given wavelengths.

The compounds in the open form displayed absorption maxima at 247-270 nm (figure 1 **a**). Compounds **5**, **13**, **14** and **15** had a second maximum at 310-330 nm, and compound **14** presented an additional maximum at 338 nm. The open forms were fluorescent with emission maxima between 425 and 435 nm.

Table 1. Optical properties of compounds **5**, **13-15**

Compound	λ_{max} Open form nm; (ε, $M^{-1}cm^{-1}$)	Photo-conversion α (λ_{irr}, nm)	λ_{max} Closed form, nm; (ε, $M^{-1}cm^{-1}$)	λ_{max} Emission open form, nm
5	257 (20000) 292 (7900)	0.83 (300) 0.72 (320) 0.33 (340) 0.10 (360) 0.07 (380)	268 (16600) 338 (8200) 431 (7600) 511 (9500)	425
13	261 (17200) 331 (5000)	0.40 (300) 0.49 (320) 0.38 (340) 0.17 (360) 0.13 (380)	278 (19000) 300 (12000) 416 (4400) 560 (14600)	435
14	271 (14800) 300 (9800) 338 (4900)	0.69 (300) 0.72 (320) 0.64 (340) 0.38 (360) 0.23 (380)	353 (7200) 428 (2600) 600 (9200)	435
15	270 (20000) 333 (5500)	0.32 (300) 0.39 (320) 0.38 (340) 0.22 (360) 0.19 (380)	300 (16400) 358 (12400) 412 (5700) 558 (15600)	434

Photochromic properties. All synthesized diarylethenes underwent reversible photochromic reactions in cyclohexane upon alternating exposure to UV (340 nm) and visible (546 nm) light. Compounds **5**, **13** and **14** displayed two isosbestic points. Compound **5** at 299 and 316 nm; compound **13** at 313 and 321 nm, and compound **14** at 311 and 332 nm. On the other hand, compound **15** had one isosbestic point at 281 nm and compound **18** lacked an isosbestic point.

Upon irradiation with UV, the color of the solutions went from colorless to red (compounds **5**, **15**, and **16**) or blue (compound **14**). The effect of substituent groups on the *N* atom was evaluated by comparison of the optical properties of the BOC, TBDMS, CH_3,[2] and CH_2COOR derivatives. The closed form (Figure 1 **b**) displayed an absorption maximum at *ca.* 560 nm for the TBDMS, CH_3 and CH_2COOR substituents. The maximum was shifted to 511 nm for the less electron rich BOC group.

Introduction of a methoxy substituent is known to affect the absorption maxima and extinction coefficient values, depending on its position on the benzothiophene ring of a diarylethene.[14] A methoxy group on position 6 (compound **15**) exerted a negligible change in the

absorption maximum and displayed a slight increase in ε compared to **13**. On the other hand, the introduction of a methoxy group in the position 5 of the indole moiety (compound **14**) introduced a red-shift of *ca.* 40 nm compared to compound **13** and a decrease of ε to 9200 $M^{-1}cm^{-1}$.

Indole derivatives as acceptors for pcFRET. The modulation of the emission of a fluorescent donor by pcFRET is based on the difference in the absorption properties of the acceptor in its different photochromic forms. Compounds **5**, **13-15** were evaluated as switchable acceptors. Figure 2 displays the absorption spectra corresponding to the open and closed forms of compound **15** and the emission spectrum of Lucifer yellow (LYC). Compound **15** displays an effective spectral overlap between its absorption and the emission of the donor (LYC) only in the closed form.

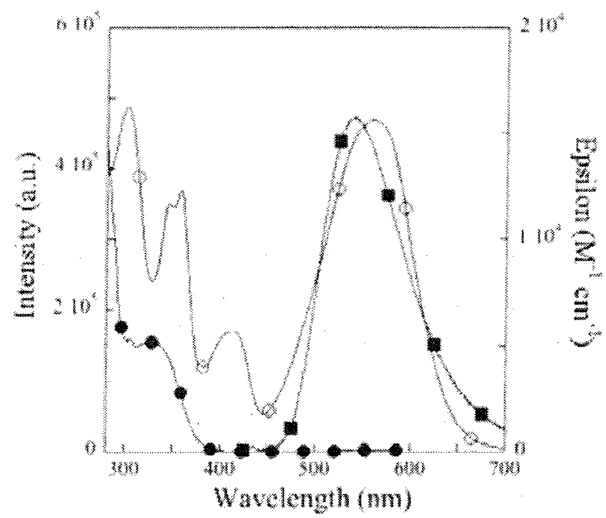

Figure 2. Spectral overlap of the open and closed forms of **15** and LYC. Open (full circles) and closed (empty circles) form extinction coefficients of **15** correspond to the right axis scale and the emission intensity of LYC (full squares) is given on the left axis.

The overlap integral J and the Förster distance R_0 were calculated for pairs consisting of the model donor, LYC and the photochromic acceptors, compounds **5**, **13-15** in their open and closed forms. Compound **14**, with a closed form displaced to the red, was additionally paired with donors sulforhodamine 101 and Nile red. In all cases, the two orders of magnitude difference in the overlap integral between the open and the closed forms demonstrated that the closed form was a competent acceptor, and the open form was not. The derived R_0 values were between 35-50 Å for the closed forms and decreased to 10-18 Å for the open forms.

Table 2. Overlap integral and Förster distances for donor - photochromic acceptor pairs in the open and closed form

Acceptor	Donor	J Open form, cm^6	R_0 Open form, Å	J Closed form, cm^6	R_0 Closed, Å
5	LYC	3.00 e-16	15	5.12 e-14	36
13	LYC	2.88e-17	10	9.82e-14	40
14	LYC	1.09 e-16	13	6.13 e-14	36
14	Sulforhodamine	1.94 e-16	18	1.06 e-13	51
14	Nile Red	1.82 e-16	17	9.06 e-14	48
15	LYC	1.88 e-16	14	9.63 e-14	40

Conclusions

The synthetic scheme using TBDMS as protective group was superior over the use of BOC for the preparation of functionalized, indole derived asymmetric diheteroarylethenes. The substitution on the indole ring at the *N*-atom had minor effects on the optical properties except for the BOC derivatives. Methoxy groups at position 5 on the indole moiety induced a red-shift of the absorption of the closed form to 600 nm and a decrease in ε. All photochromic compounds prepared in this work constitute good acceptors that can switch *on* and *off* the FRET process in pcFRET.

Experimental Section

General Procedures. Melting points were determined with a Fisher Jones apparatus and are uncorrected. NMR measurements were carried out on a Bruker 200 MHz AM, 400 MHz, 500 MHz AMX, Mercury 300 MHz (Varian) or on a INOVA 500 MHz (Varian) NMR spectrometer. Chemical shifts are in ppm (internal TMS) and coupling constants in Hz. All reactions were monitored by thin-layer chromatography on Merck silica gel plates (60F-254). Column chromatography was performed on silica gel (Merck, 230-400 mesh ASTM). The purities of all final compounds were checked HPLC analysis on a Waters system fitted with a MZ-Semipreparative Kromasil 100 Sil 5 µm silica column (25 cm long, 10 mm internal diameter). ESI and HRMS were measured on an APEX IV 7 Tesla-Fourier Transform Ion Cyclotron Resonance (FTICR)- Mass spectrometer (Bruker) or on a TSQ 7000 Triple-Stage-Quadrupol-Instrument (Finnigan) with Electrospray-Ionisation. Elementary analyses were measured with a Leco CHN2000 analyser with burn unit MICRO U/D (Heraeus). Absorption and fluorescence spectra were measured with a UVIKON 943 Double Beam UV/Vis absorption spectrophotometer and a Perkin Elmer LS50B fluorescence spectrophotometer, respectively. Photoirradiation was carried out using a Superlite SUV-DC-P system incorporating a 200W DC Super-Pressure short arc lamp coupled to a light guide for high UV transmission and an

electronic timer for exposure time control (Lumatec GmbH, Munich, Germany). Monochromic light was obtained by passing the light a band-pass filter ($\Delta\lambda_{1/2}$=10 nm). The photoconversions were determined with an Ocean Optics fiber optics spectrometer system with a cuvette holder specially modified to allow simultaneous photoconversion and spectral monitoring. Excitation for absorption and fluorescence was with a DT1000A deuterium/tungsten lamp, and detection was with a SD2000 series dual fiber optics spectrometer optimized for detection in the 250-800 nm spectral region.

FRET Methods. , the critical Förster distance for 50% FRET efficiency, is defined by $R_oR_o^6 = 8.785 \cdot 10^{-5} \kappa^2 \Phi_D J n^{-4}$ units, nm^6) where Φ_D is the quantum yield of the donor in the absence of acceptor, n is the refractive index of the medium, κ^2 is the orientation factor between donor and acceptor (here assumed to be 2/3, the value corresponding to rapid and isotropic reorientation of donor and acceptor during the excited state), and J is the spectral overlap integral between donor and acceptor, given by $J = \int F_\lambda^D \varepsilon_\lambda^A \lambda^4 d\lambda$, where F_λ is the normalized donor fluorescence spectrum and ε_λ is the wavelength-dependent molar extinction coefficient (M^{-1} cm^{-1}) of the acceptor. For an isolated donor-acceptor pair, the FRET efficiency E varies according to $E = [1 + (r_{DA}/R_o)^6]^{-1}$.

Materials. 2-methyl-*1H*-indole (**1**), 5-methoxy-2-methyl-*1H*-indole (**8**), are commercially available and were obtained from Aldrich Chem. Co. Compounds **7**[15] and **16**[14] were prepared as previously described.

3-Iodo-2-methyl-1*H*-indole (2). A solution of I_2 (9.7 g, 38 mmol) in DMF (65 ml) was added dropwise to a solution of **1** (5.0 g, 38 mmol) and KOH (5.3 g, 95 mmol) in DMF (80 ml) at room temperature and stirred for 30 min. The reaction mixture was poured into ice and water (1 l) containing ammonia (0.5 %) and sodium metabisulphite (0.1 %). The orange-white precipitate was filtered and washed with cold water. The obtained 3-iodo-2-methyl-1*H*-indole **2** (9.3 g, 36 mmol, 95%) was used without further purification. M.p: 82 °C (lit:[16] 83-84 °C). ^{1}H-NMR (400 MHz, $CDCl_3$): δ 8.16 (1H, bs, NH), 7.35 (1H, m), 7.25 (1H, m), 7.16 (2H, m), 2.48 (3H, s).

***tert*-Butyl 3-iodo-2-methyl-1*H*-indole-1-carboxylate (3).** Compound **2** (1.57 g, 6.1 mmol) was dissolved in dichloromethane (150 ml) and treated with di-*tert*-butyldicarbonate (1.57 g, 7.2 mmol), triethylamine (2.7 ml, 19 mmol), DMAP (80 mg, 0.66 mmol) and the reaction mixture was stirred at room temperature for 30 min. The solution was washed twice with sodium metabisulphite (5%, 50 ml each time), dried over Na_2SO_4 and concentrated under reduced pressure. Chromatography over silica gel (hexane:ethyl acetate = 8:2) gave **3** (1.99 g, 5.6 mmol, 90%) as a colorless solid. M.p 55-56 ° C. ^{1}H-NMR (400 MHz, $CDCl_3$): δ 8.06 (1H, dd, J = 7.1 and 2.2 Hz), 7.36 (1H, dd, J = 6.5 and 2.7 Hz), 7.27-7.30 (2H, m), 2.72 (3H, s), 1.69 (9H, s). ^{13}C-NMR (50 MHz, $CDCl_3$): δ 149.8, 138.2, 136.0, 131.2, 124.5, 123.2, 120.9, 115.4, 84.3, 71.4, 28.2 (3C), 17.9. Anal. Calcd. for $C_{14}H_{16}INO_2$ (357.19) C 47.08, H 4.52, N 3.92. Found: C 47.02,

H 4.41, N 3.85. MS (ESI): m/z (%): 357 ($M^{+\cdot}$, 43); 301 (100); 257 (80); 130 (15), 57 (97).

3-(2,3,3,4,4,5,5-Heptafluorocyclopent-1-enyl)-1-(*t*-butoxycarbonyl)-2-methyl-1*H*-indole (4). A solution of *n*-BuLi in hexane (1.6 M, 1.0 ml, 1.6 mmol) was added to a stirred solution of **3** (0.50 g, 1.4 mmol) in anhydrous THF (6 ml) at -20 °C under argon atmosphere. After the addition was complete, the resulting mixture was cooled to -78 °C and octafluorocyclopentene (0.19 ml, 1.4 mmol) was added in a single portion. The mixture was stirred for 1 h at -78 ° C. The mixture was allowed to warm to room temperature and hydrolyzed with an aqueous HCl (1 N, 7 ml) solution. The mixture was extracted with ethyl acetate (4 x 5 ml). The combined organic layers were washed with H_2O and saturated aqueous NaCl solution, dried over Na_2SO_4 and concentrated under reduced pressure. The crude product was purified by flash column chromatography on silica with hexane and followed by HPLC (silica gel column, hexane) to give **4** as a white solid (250 mg, 0.59 mmol, 42 %). M.p.: 74-75 °C. ^{1}H-NMR (500 MHz, $CDCl_3$): δ 8.14 (1H, d, J = 8.3 Hz), 7.42 (1H, d, J = 7.3 Hz), 7.27-7.35 (2H, m), 2.55 (3H, s), 1.71 (9H, s). ^{13}C-NMR (125 MHz, $CDCl_3$): δ 149.9, 139.3, 135.9, 127.0, 124.6, 123.6, 118.7, 115.6, 85.1, 28.2 (3C), 15.2. (Resonances of the *C*-atoms of the fluorinated cyclopentene moiety could not be observed due to low intensity and extensive splitting). Anal. Calcd. for $C_{19}H_{16}F_7NO_2$ (423.33): C 53.91; H 3.81. Found: C 53.70; H 3.66. HRMS: Calcd. 423.1069. Found: 423.1069. MS (ESI) m/z (%): 423 ($M^{+\cdot}$, 22), 367 (48), 323 (66), 301 (24), 257 (22), 57 (100).

3-[3,3,4,4,5,5-Hexafluoro-2-(2-methylbenzo[*b*]thien-3-yl)-cyclopent-1-enyl]-1-(*t*-butoxycarbonyl)-2-methyl-1*H*-indole (5). A solution of *n*-BuLi in hexane (1.6 M, 0.77 ml, 1.2 mmol) was added to a stirred solution of **3** (200 mg, 0.56 mmol) in anhydrous THF (3 ml) at -78 °C under nitrogen atmosphere. The resulting mixture was stirred for 30 min at -78 °C and a solution of **7** (200 mg, 0.61 mmol) in anhydrous THF (1 ml) was added. After the addition was complete, the mixture was allowed to return to room temperature and it was hydrolyzed with an aqueous HCl (1N, 5 ml) solution. The mixture was extracted with ethyl acetate (3 x 5 ml). The resulting organic phase was washed with H_2O and saturated aqueous NaCl solution, dried over Na_2SO_4 and concentrated under reduced pressure. The crude product was purified by flash column chromatography on silica with hexane/ethyl acetate 98:2 to give **5** as a slightly yellow solid (70 mg, 0.13 mmol, 20 %). M.p.: 71-72 °C. ^{1}H-NMR (300 MHz, $CDCl_3$) (323 K): δ 8.01 (1H, *d*, J = 7.5 Hz), 7.67 (1H, d, J = 7.0 Hz), 7.60 (1H, d, J = 6.5 Hz), 7.50 (1H, d, J = 7.4 Hz), 7.17-7.27 (4H, m), 2.36-2.31 (6H, bs). Anal. calcd. for $C_{28}H_{23}F_6NO_2S$ (551.55): C 60.97, H 4.20, N 2.54. Found: C 60.74, H 3.96, N 2.62. HRMS Calcd.: 551.1354; found: 551.1354. MS (EI) m/z (%): 551 ($M^{+\cdot}$, 13), 495 (22), 451 (14), 57 (100).

3-(2-Butyl-3,3,4,4,5,5-hexafluorocyclopent-1-enyl)-2-methylbenzo[*b*]thiophene (6). ^{1}H-NMR (400 MHz, $CDCl_3$): δ 7.78 (1H, d, J = 7.8 Hz), 7.49 (1H, d, J = 7.9 Hz), 7.39 (1H, m), 7.34 (1H, m), 3.81 (1H, m), 3.65 (1H, m), 2.51 (3H, s), 1.46 (2H, m), 1.18 (2H, m), 0.73 (3H, t, J = 8 Hz).

1-(*tert*-Butyldimethylsilanyl)-2-methyl-1*H*-indole (9). Sodium hydride (350 mg, 9.2 mmol, mineral oil suspension 50%) was added in portions to a stirred solution of **1** (1.0 g, 7.6 mmol) in anhydrous THF (15 ml) and the mixture was stirred for 10 min. *tert*-Butyl(chloro)dimethylsilane (1.4 g, 9.2 mmol) was added and the mixture was stirred for 12 h at room temperature under

nitrogen atmosphere. The reaction was quenched with water (10 ml). The mixture was extracted with ethyl acetate (2 x 5ml). The organic layer was washed with saturated aqueous NaCl solution (10 ml), dried over Na_2SO_4, filtered and concentrated under reduced pressure. The residue was purified by flash column chromatography on silica (cyclohexane) to give **9** as a colorless oil (1.67 g, 6.8 mmol, 89%). ^{1}H-NMR (200 MHz, $CDCl_3$): δ 7.46-7.53 (2H, m), 7.03-7.08 (2H, m), 6.34 (1H, s), 2.49 (3H, s), 0.97 (9H, s), 0.67 (6H, s). ^{13}C-NMR (50 MHz, $CDCl_3$): δ 142.7, 142.0, 131.3, 120.3, 119.6, 119.1, 114.1, 106.1, 26.8 (3C), 20.6, 17.5, -0.5 (2C).

3-Bromo-1-(*tert*-butyldimethylsilanyl)-2-methyl-1*H*-indole (11). *N*-Bromosuccinimide (145 mg, 0.81 mmol) was added to a solution of **9** (200 mg, 0.81 mmol) in anhydrous THF (5 ml) at -78 ° C. After 2 h, the mixture was allowed to warm up to room temperature. The mixture was evaporated under reduced pressure. The residue was purified by flash column chromatography (silica, cyclohexane) to give **11** as a white solid (180 mg, 0.56 mmol, 68%). ^{1}H-NMR (200 MHz, $CDCl_3$): δ 7.48-7.52 (2H, m), 7.18-7.14 (2H, m) 2.53 (3H, s), 1.00 (9H, s), 0.69 (6H, s). ^{13}C-NMR (50 MHz, $CDCl_3$): δ 140.9, 138.4, 130.0, 121.6, 120.4, 118.4, 114.3, 95.9, 26.7 (3C), 20.5,15.5, -0.3 (2C).

1-(*tert*-Butyldimethylsilanyl)-3-[3,3,4,4,5,5-hexafluoro-2-(2-methylbenzo[*b*]thien-3-yl)-cyclopent-1-enyl]-2-methyl-1*H*-indole (13). A solution of *n*-BuLi in hexane (1.6 M, 0.53 ml, 0.61 mmol) was added to a stirred solution of **11** (180 mg, 0.56 mmol) in anhydrous THF (3 ml) at -78 °C under argon atmosphere. The resulting orange solution was stirred for 30 min at -78 °C and a solution of 7 (210 mg, 0.61 mmol) in anhydrous THF (1 ml) was added. After 30 min at -78 °C, the mixture was allowed to warm to room temperature and it was hydrolyzed with an aqueous HCl (1N, 5 ml) solution. The mixture was extracted with ethyl acetate (2 x 5 ml). The combined organic layers were washed with H_2O and saturated aqueous NaCl solution, dried over Na_2SO_4 and concentrated under reduced pressure. The crude product was purified by flash column chromatography on silica with hexane/ethyl acetate 98:2 to give a slightly yellow solid (125 mg, 0.22 mmol 40 %). Purification by HPLC (silica 60, hexane) gave **13** as a white solid (115 mg, 0.2 mmol, 37%). M.p.: 162-163 °C. ^{1}H-NMR (300 MHz, $CDCl_3$): δ 7.43-7.64 (4H, m), 7.06-7.24 (4H, m) 2.27 (3H, bs), 1.98 (3H, s), 0.60 (9H, s), 0.54 (6H, s). ^{13}C-NMR (75 MHz, $CDCl_3$): δ 142.8, 142.2, 141.8, 138.0, 129.0, 124.3, 124.1, 122.2, 121.7, 121.5, 120.7, 120.6, 119.1, 119.0, 118.9, 114.2, 26.3 (3C), 20.5, 15.8, 15.1, -0.2 (2C). (Resonances of the *C*-atoms of the fluorinated cyclopentene moiety could not be observed due to low intensity and extensive splitting). Anal. Calcd. for $C_{29}H_{29}F_6NSSi$ (565.69): C 61.57, H 5.17; found: C 61.51, H 4.95. MS (ESI) m/z (%): 565 ($M^{+\cdot}$, 68), 509 (22), 73 (100). HRMS. Calcd.: 565.1694. Found: 565.1694.

1-(*tert*-Butyldimethylsilanyl)-3-[3,3,4,4,5,5-hexafluoro-2-(6-methoxy-2-methyl-benzo[*b*]thien-3-yl)-cyclopent-1-enyl]-2-methyl-1*H*-indole (15). A solution of *n*-BuLi in hexane (1.6 M, 0.77 ml, 0.88 mmol) was added to a stirred solution of **11** (260 mg, 0.80 mmol) in anhydrous THF (3 ml) at -30 °C under argon atmosphere. The resulting mixture was stirred for 30 min at -30 °C and the mixture was cooled at – 78 ° C. A solution of **16** (300 mg, 0.80 mmol) in anhydrous THF (1 ml) was added. After 30 min at -78 °C, the mixture was allowed to warm to room temperature and it was hydrolyzed with an aqueous HCl (1N, 5 ml) solution. The mixture

was extracted with ethyl acetate (2 x 5 ml). The combined organic layers were washed with H_2O and saturated aqueous NaCl solution, dried over Na_2SO_4 and concentrated under reduced pressure. The crude product was purified by flash column chromatography on silica with hexane/ethyl acetate 98:2 to give a white solid (180 mg, 0.30 mmol, 38 %). Purification by HPLC (silica 60, hexane) gave **15** as a white solid (170 mg, 0.29 mmol, 36 %). M.p.: 152-153 °C. ^{1}H-NMR (300 MHz, $CDCl_3$): δ 7.61 (1H, d, J = 8.1 Hz), 7.44 (1H, d, J = 8.3 Hz), 7.06-7.13 (4H, m), 6.81 (1H, bs), 3.80 (3H, s), 2.19 (3H, bs), 1.97 (3H, s), 0.63 (9H, s), 0.55 (6H, s). ^{13}C-NMR (75 MHz, $CDCl_3$): δ 157.1, 142.8, 141.8, 139.4, 132.1, 129.0, 122.9, 121.5, 120.8, 119.1, 119.0, 118.9, 114.2, 114.0, 105.7, 104.6, 55.5, 26.4 (3C), 20.5, 15.8, 15.0, -0.1 (2C). (Resonances of the *C*-atoms of the fluorinated cyclopentene moiety could not be observed due to low intensity and extensive splitting). Anal calcd for $C_{30}H_{31}F_6NOSSi$ (595.71): C 60.49, H 5.25. Found: C 60.64, H 5.00. MS (EI) m/z (%): 565 ($M^{+\cdot}$, 100), 539 (25), 538 (26), 73 (76). HRMS. Calcd: 595.1800. Found: 595.1800.

1-(*tert*-Butyldimethylsilanyl)-2-methyl-5-methoxy-1*H*-indole (10). Sodium hydride (130 mg, 3.7 mmol, mineral oil suspension 50%) was added in portions to a stirred solution of **8** (0.50 g, 3.1 mmol) in anhydrous THF (10 ml) and the mixture was stirred for 10 min. *tert*-Butyl(chloro)dimethylsilane (0.56 g, 3.7 mmol) was added and the mixture was stirred for 12 h at room temperature under nitrogen atmosphere. The reaction was quenched with water (10 ml). The mixture was extracted with ethyl acetate (2 x 5ml). The combined organic layers were washed with saturated aqueous NaCl (10 ml) solution, dried over Na_2SO_4, filtered and concentrated under pressure. The residue was purified by flash column chromatography on silica (cyclohexane) to give **10** as colorless oil (635 mg, 2.3 mmol, 74%). ^{1}H-NMR (200 MHz, $CDCl_3$): δ 7.37 (1H, d, J = 9 Hz), 6.95 (1H, d, J = 2.4 Hz), 6.70 (1H, dd, J = 9 and 2.4 Hz) 6.26 (1H, s), 3.83 (3H, s), 2.46 (3H, s), 0.95 (9H, s), 0.64 (6H, s).

3-Bromo-1-(*tert*-butyldimethylsilanyl)-2-methyl-5-methoxy-1*H*-indole (12). *N*-Bromosuccinimide (400 mg, 2.3 mmol) was added to a solution of **10** (635 mg, 2.3 mmol) in anhydrous THF (10 ml) at -78 ° C. After 2 h, the mixture was allowed to warm up to room temperature. The mixture was concentrated under reduced pressure. The crude residue was purified by flash column chromatography (silica, cyclohexane) to give **12** as a white solid (710 mg, 2.0 mmol, 87%). ^{1}H-NMR (200 MHz, $CDCl_3$): δ 7.36 (1H, d, *J* = 9.0 Hz), 6.91 (1H, d, *J* = 2.4 Hz), 6.76 (1H, dd, *J* = 9.0 and 2.4 Hz), 3.88 (3H, s), 2.49 (3H, s), 0.97 (9H, s), 0.65 (6H, s) ^{13}C-NMR (50 MHz, $CDCl_3$): δ 154.6, 139.1, 135.6, 130.6, 115.1, 111.4, 100.1, 95.5, 55.7, 26.7 (3C), 20.4, 15.5, -0.4 (2C).

1-(*tert*-Butyldimethylsilanyl)-3-[3,3,4,4,5,5-hexafluoro-2-(2-methylbenzo[*b*]thien-3-yl)-cyclopent-1-enyl]-2-methyl-5-methoxy-1*H*-indole (14). A solution of *n*-BuLi in hexane (1.0 M, 0.93 ml, 0.93 mmol) was added to a stirred solution of **12** (300 mg, 0.85 mmol) in anhydrous THF (10 ml) at -30 °C under argon atmosphere. The resulting orange mixture was stirred for 30 min at -30 °C and the reaction was cooled at -78 °C. A solution of **7** (290 mg, 0.85 mmol) in anhydrous THF (2 ml) was added. After 30 min at -78 °C, the mixture was allowed to warm up to room temperature and it was hydrolyzed with an aqueous HCl (1N, 5 ml) solution. The

mixture was extracted with ethyl acetate (2 x 5 ml). The combined organic layers were washed with H_2O and saturated aqueous NaCl solution, dried over Na_2SO_4 and concentrated under reduced pressure. The crude product was purified by flash column chromatography on silica with cyclohexane/ethyl acetate 98:2 to give **14** as a yellow solid (270 mg, 0.45 mmol 53 %). M.p.: 167-168 °C. ^{1}H-NMR (500 MHz, $CDCl_3$): δ 7.65 (1H, bs), 7.22-7.31 (4H, m), 7.01 (1H, bs) 6.71 (1H, d, J = 8.5 Hz), 3.76 (3H, s), 2.24 (3H, bs), 1.98 (3H, bs), 0.61 (9H, s), 0.53 (6H, s). ^{13}C-NMR (125 MHz, $CDCl_3$): δ 154.6, 143.5, 142.3, 138.2, 136.7, 129.7, 124.4, 124.2, 122.4, 122.3, 121.8, 114.9, 111.1, 101.1, 55.7, 26.4 (3C), 20.5, 16.0, -0.1 (2C). (Resonances of the *C*-atoms of the fluorinated cyclopentene moiety could not be observed due to low intensity and extensive splitting). MS (EI) m/z (%): 596 (M+H$^+$, 10), 480 (100).

3-[3,3,4,4,5,5-Hexafluoro-2-(2-methylbenzo[*b*]thien-3-yl)-cyclopent-1-enyl]-2-methyl-1*H*-indole (17). A solution of tetrabutylammonium fluoride (TBAF) in THF (1M, 0.11 ml, 0.11 mmol) was added to a stirred solution of **13** (60 mg, 0.11 mmol) in THF (1 ml), under argon atmosphere. After the solution was stirred for 20 min at room temperature, it was poured into a saturated solution of Na_2CO_3 (2 ml) and extracted with CH_2Cl_2 (3 x 2 ml). The organic layers were combined and washed with H_2O (2 ml), dried over Na_2SO_4, and concentrated under reduced pressure. The residue was subjected to flash column chromatography on silica gel (cyclohexane/ethyl acetate 8:2) to give 40 mg (0.09 mmol, 84%) of the desired compound. Compound **17** was used immediately in the next reaction. ^{1}H-NMR (200 MHz, $CDCl_3$): δ 7.97 (1H, bs), 7.59-7.69 (3H, m), 7.23-7.28 (2H, m), 7.07-7.18 (3H, m), 2.24 (3H, s), 1.94 (3H, s).

Ethyl {3-[3,3,4,4,5,5-hexafluoro-2-(2-methylbenzo[*b*]thien-3-yl)-cyclopent-1-enyl]-2-methyl-1*H*-indol-1-yl}acetate (18). NaH (2mg, 0.06 mmol, mineral oil suspension, 50%) was added to a stirred solution of **17** (20 mg, 0.04 mmol) in DMF (0.5 ml) under N_2. After stirring for 30 min, the mixture was cooled and one drop of ethyl bromoacetate was added. The resulting red-brown solution was stirred for 2.5 h and diluted with 5 ml of ethyl acetate. The organic layer was washed with H_2O (3 x 3 ml) and saturated NaCl solution, dried over N_2SO_4 and concentrated to give red oil. The oil was purified by flash column chromatography on silica (cyclohexane/ethyl acetate 8:2) to give **18** (8 mg, 0.01 mmol, 34%) as a slightly yellow solid. ^{1}H-NMR (200 MHz, $CDCl_3$): δ 7.62-7.69 (3H, m), 7.25-7.31 (3H, m), 7.10-7.15 (2H, m), 4.63 (2H, s), 4.06 (2H, q, J = 7.1 Hz), 2.19 (3H, s), 1.90 (3H, s), 1.09 (3H, t, J = 7.1 Hz).

{3-[3,3,4,4,5,5-Hexafluoro-2-(2-methylbenzo[*b*]thien-3-yl)-cyclopent-1-enyl]-2-methyl-1*H*-indol-1-yl}acetic acid (19). Compound **18** was dissolved in THF (1 ml), an aqueous solution of NaOH (1M, 0.5 ml, 0.5 mmol) was added, and the mixture was stirred under reflux for 1 h. The reaction mixture was cooled to room temperature and diluted with H_2O. After acidification of the solution to pH 1 using concentrated HCl the suspension was extracted with CH_2Cl_2 (2 x 2 ml) and the organic phases were dried over Na_2SO_4 and concentrated under reduced pressure. The product was purified by preparative thin layer chromatography on reverse phase silica (RP18) with ethyl acetate/2-propanol/H_2O 4:3:2 as a solvent to give **19** (4 mg, 0.008 mmol, 60%) as a slightly yellow solid. ^{1}H-NMR (200 MHz, $CDCl_3$): δ 7.62-7.66 (3H, m), 7.26 (3H, m), 7.13-7.15 (2H, m), 4.65 (2H, s), 2.18 (3H, s), 1.88 (3H, s).

Acknowledgements

The authors would like to thank Dr. Leonardo Erijman and Dr. Thomas Jovin for careful reading of the manuscript. E.A.J.-E. is indebted to the Agencia Nacional de Promoción de la Ciencia y Tecnología (ANPCyT), Fundación Antorchas, Consejo Nacional de Investigaciones Científicas y Técnicas (CONICET), Secretaría de Ciencia, Tecnología e Innovación Productiva (SECyT), Germany-Argentine DLR-BMBF-SECyT, and the Universidad de Buenos Aires (UBA) for financial support. E.A.J.-E. is recipient of the grant I/77 897 from the Volkswagen Foundation for collaborative work on pcFRET with Dr. Thomas Jovin (MPIBPC-Goettingen, Germany).

References

1. Hirshberg, *Compt. Rend.* **1950**, *231*, 903.
2. Irie, M. *Chem. Rev.* **2000**, *100*, 1685.
3. Yagi, K.; Irie, M. *Bull. Chem. Soc. Jpn.* **2003**, *76*, 1625.
4. Giordano, L.; Jovin, T. M.; Irie, M.; Jares-Erijman, E. A. *J. Am. Chem. Soc.* **2002**, *124*, 7481.
5. Jares-Erijman, E. A.; Jovin, T. M. *Nat. Biotechnol.* **2003**, *21*, 1387.
6. Hanazawa, M.; Sumiya, R.; Horikawa, Y.; Irie, M. *J. Chem. Soc., Chem. Commun.* **1992**, 206.
7. Greene, T. W.; Wuts, P. G. M. *Protective Goups in Organic Synthesis*. Wiley-Interscience: New York, 3rd Edn, 1999.
8. Dhanak, D.; Reese, C. B. *J. Chem. Soc., Perkin Trans. 1* **1986**, 2181.
9. Witulski, B.; Buschmann, N.; Bergstrasser, U. *Tetrahedron* **2000**, *56*, 8473.
10. Bodwell, G. J.; Li, J. *Org. Lett.* **2002**, *4*, 127.
11. Amat, M.; Hadida, S.; Sathyanarayana, S.; Bosch, J. *J. Org. Chem.* **1994**, *59*, 10.
12. Cross, P. E.; Dickinson, R. P.; Parry, M. J.; Randall, M. J. *J. Med. Chem.* **1986**, *29*, 1637.
13. Bell, M. R.; Dambra, T. E.; Kumar, V.; Eissenstat, M. A.; Herrmann, J. L.; Wetzel, J. R.; Rosi, D.; Philion, R. E.; Daum, S. J.; Hlasta, D. J.; Kullnig, R. K.; Ackerman, J. H.; Haubrich, D. R.; Luttinger, D. A.; Baizman, E. R.; Miller, M. S.; Ward, S. J. *J. Med. Chem.* **1991**, *34*, 1099.
14. Frigoli, M.; Mehl, G. H. *Chem.- Eur. J.* **2004**, *10*, 5243.
15. Nakashima, H.; Irie, M. *Polymer J.* **1998**, *30*, 985.
16. Orazi, O.; Corral, R. A.; Bertorello, H. E. *J. Org. Chem.* **1965**, *30*, 1101.